Electronic Supplementary Material (ESI) for CrystEngComm.

Supplementary Information

Novel solid forms of lonidamine: crystal structures and physicochemical properties

Lucy K. Mapp,[a,b] Simon J. Coles,[b] Srinivasulu Aitipamula[a]*

[a]Crystallization and Particle Sciences, Institute of Chemical and Engineering Sciences, A*STAR (Agency for Science Technology and Research), 1 Pesek Road, Jurong Island, Singapore, 627833. E-mail: srinivasulu_aitipamula@ices.a-star.edu.sg

[b]Chemistry, Faculty of Natural and Environmental Sciences, University of Southampton, University Road, Southampton, SO17 1BJ, UK.

1. PXRD Analysis of Lonidamine (LON) Polymorphs

The reported work of Benetollo[1] and the patent of Xinmin[2] used alternative naming schemes for the polymorphs. Analysis of the reported data in conjunction with our own findings allows these to be corroborated.

1.1 PXRD patterns for α-LON calculated from the crystal structure and the reported pattern for Form I taken from the patent.

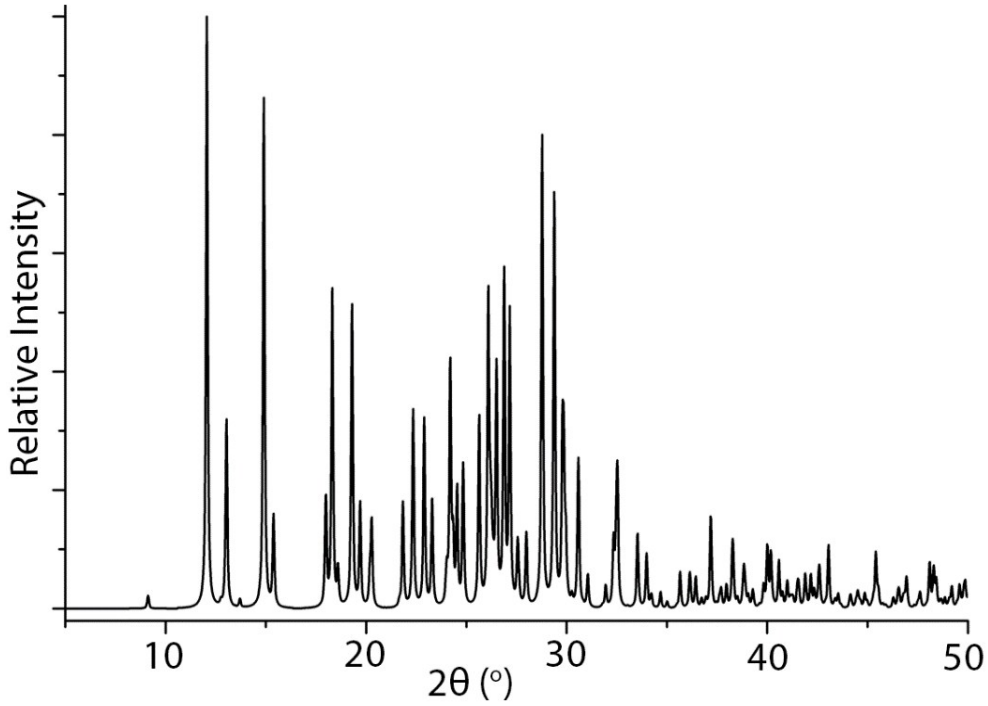

Figure 1. Form I PXRD pattern calculated from crystal structure data of α-LON.

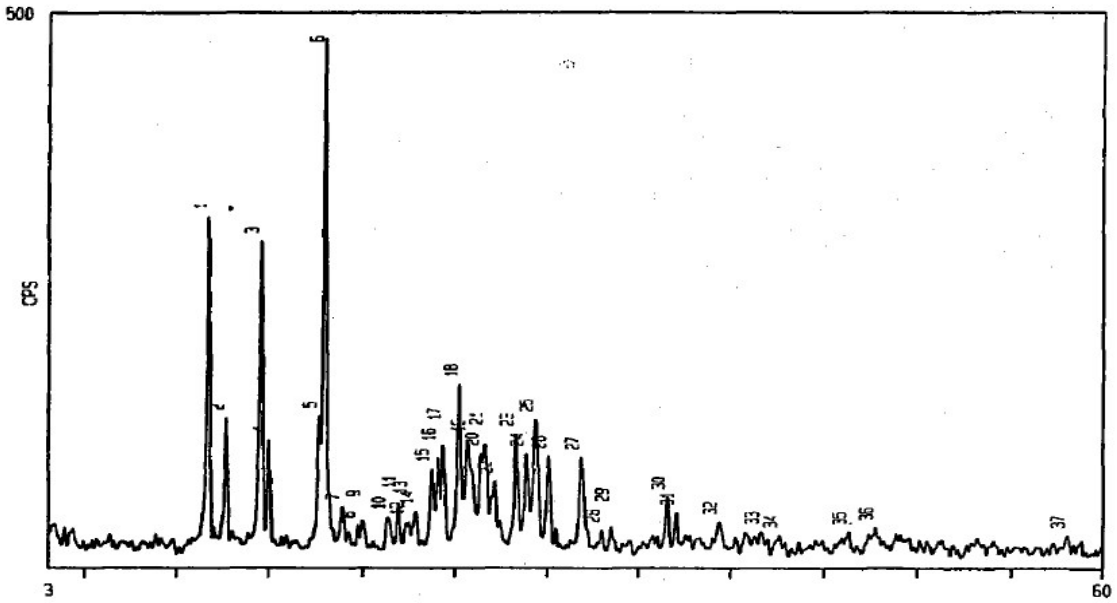

Figure 2. Form I reported PXRD pattern taken from patent by Xinmin *et al.*

1.1 PXRD patterns for β-LON calculated from the crystal structure and the reported pattern for form II taken from the patent.

Reported cell parameters for the latter are: a = 7.7117 Å, b = 8.1384 Å, c = 11.987 Å, α = 106.17 °, β = 93.05 °, γ = 96.96 °, which match the experimental data (Table 5.1.1)

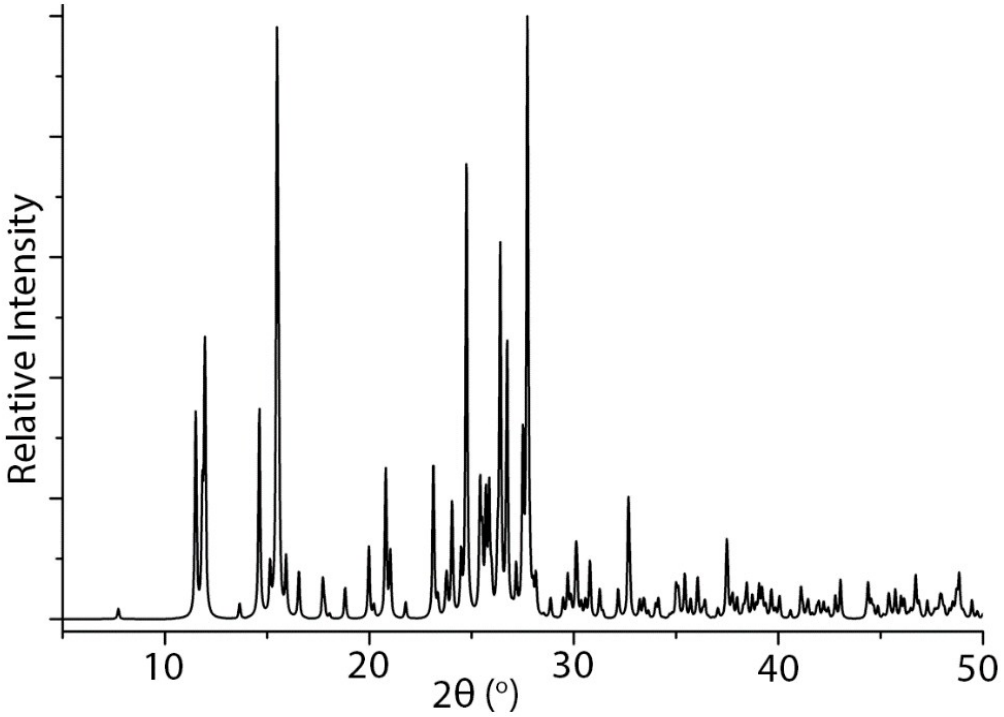

Figure 3. PXRD pattern calculated from crystal structure of β-LON.

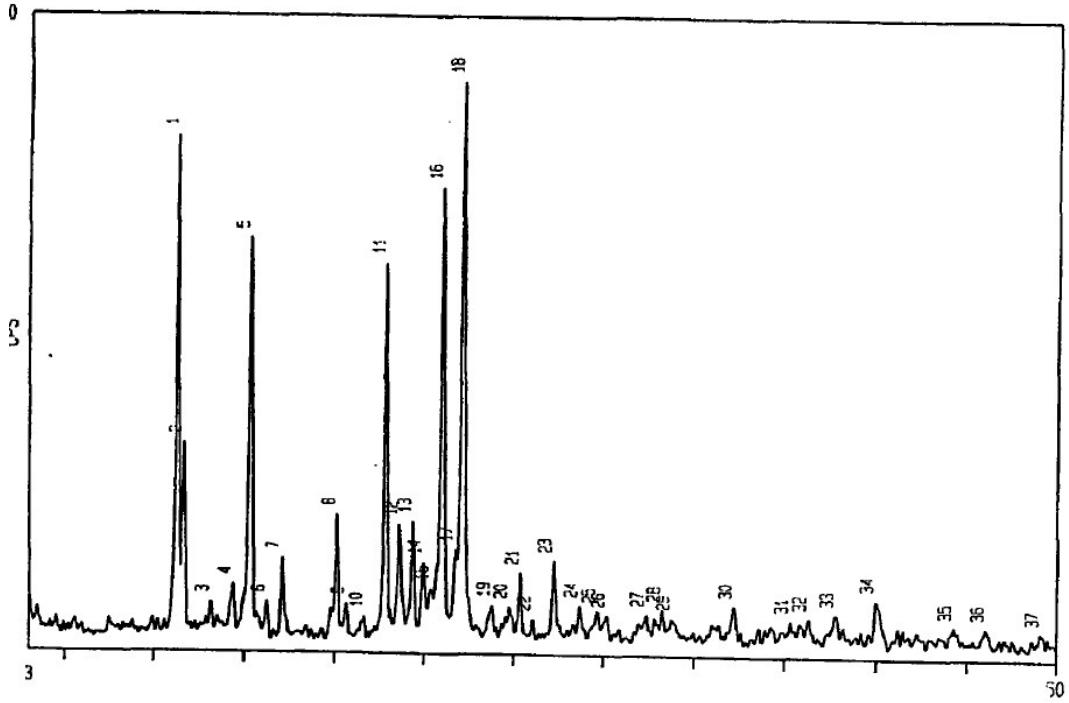

Figure 4. Reported PXRD pattern for Form II from Xinmin et al.

1.3 PXRD patterns for form III taken from the patent (below).

Reported cell parameters are: a = 5.2879 Å, b = 8.1754 Å, c = 16.768 Å, α = 80.09 °, β = 89.89 °, γ = 80.65 °. These are different to those experimentally determined for α- and β-LON.

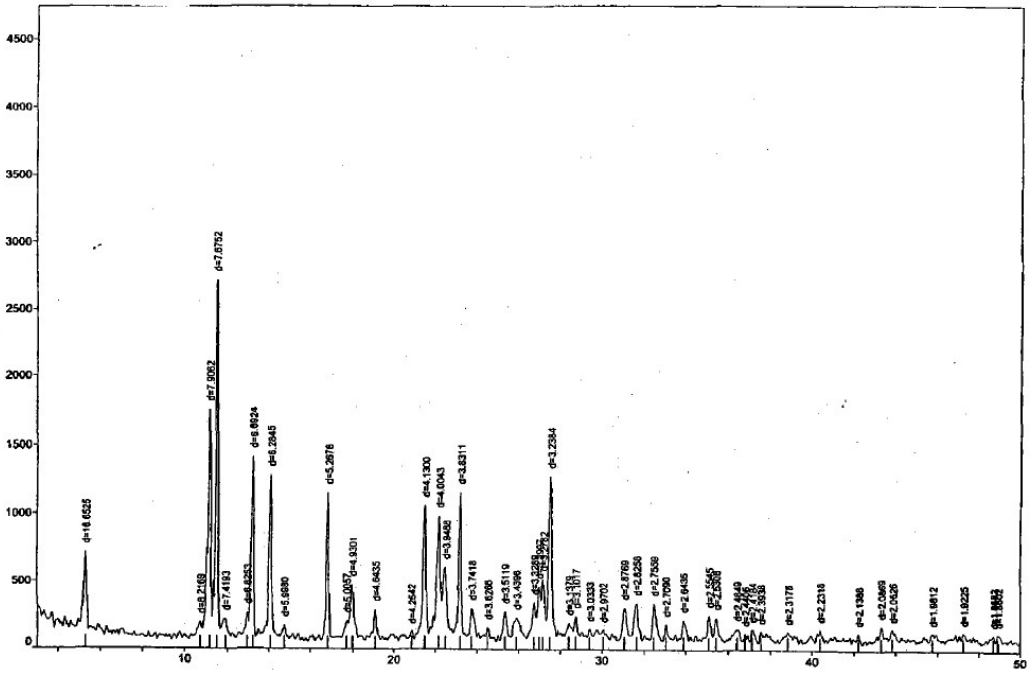

Figure 5. Reported PXRD pattern for LON Form III from patent by Xinmin et al.

1.4 Reported peaks for PXRD patterns

Table 1.1. Reported peaks from powder X-ray diffraction patterns for forms I, II and III as reported by Xinmin et al. in patent no CN101735151 B

FORM I		FORM II		FORM III	
2θ	**d**	**2θ**	**d**	**2θ**	**d**
11.7	7.5	11.3	7.8	5.3	16.6
12.7	6.1	11.7	7.6	11.1	7.9
14.5	5.9	15.3	5.8	11.5	7.7
15.0	5.0	20.1	4.4	13.2	6.7
17.7	4.9	22.9	3.9	14.0	6.28
17.9	3.7	26.0	3.4	16.8	5.3
24.1	3.5	27.1	3.3	21.5	4.1
25.2	3.5	32.2	2.8	22.2	4.0
25.6	3.4			22.5	3.9
26.4	3.3			23.2	3.8
27.1	3.2			27.5	3.2
28.3	3.1				
29.4	3.0				
30.0	3.0				
31.9	2.8				

1.5 DSC Data

Xinmin *et al*[2] have reported endotherms of form I at 211.0°C and form III and 211.3°C, whilst Benetollo *et al*[1] have reported melting points of 211.6-212.2°C (α) and 208.5-209.5°C (β).

2. Characterization of the bulk powder

A PXRD comparison of calculated patterns from experimental crystal structures and the bulk powder material used in experiments revealed that the bulk sample used for all experimental work contains a mixture of the two forms however, the β-form predominates. DSC profile shows an endotherm at 209.4°C, it is this form for which some crystalline material is present and identified by SCXRD. PXRD patterns (Figure 6) however indicate some peaks belonging to the α-form as well as those for the β-form, indicating a mixture of the two forms.

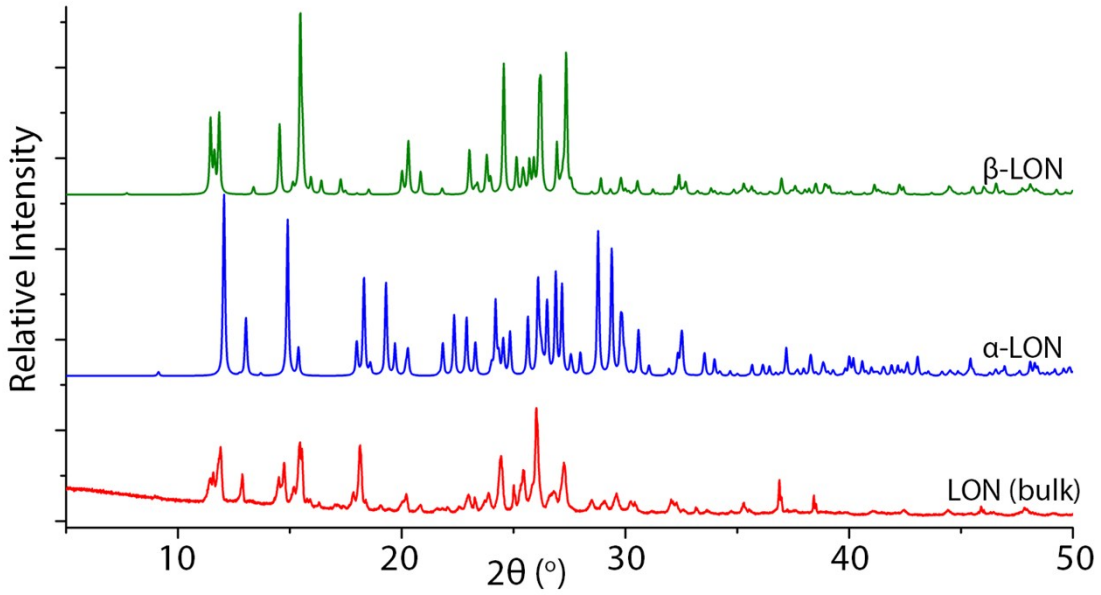

Figure 6. PXRD comparison of bulk LON (Junda Chemicals) with calculated patterns from crystal structures of the two polymorphs.

3. Control of Polymorphs

Rotary evaporation of solutions was employed to investigate the conditions (solvents) required to obtain the different forms. By quickly remove solvent in this way, thermodynamics had less influence on the resultant form and a purer sample was possible. Rotary evaporation of LON dissolved in ethyl acetate, ethyl acetate-H_2O and 1,4-dioxane solvents produced the α- form, whilst methanol produced the β-form (Figure 7). Solution crystallisation experiments produced α-LON from ethyl acetate and an ethyl acetate-acetonitrile solvent mix. β-LON was obtained from MeOH, THF, DMF, DMSO, formic acid and a MeOH-acetonitrile solvent mix.

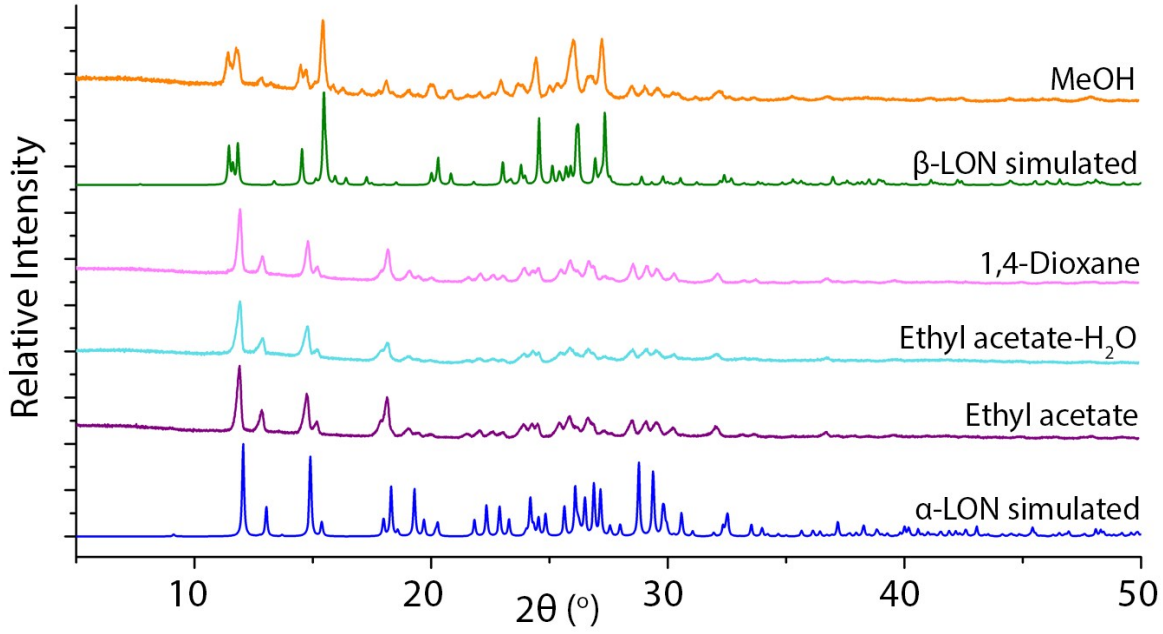

Figure 7. PXRD comparison of solids produced from rotary evaporation of solutions of LON with various solvents and calculated patterns from the crystal structures of α- and β-LON.

4. CSD Analysis

In order to understand the preferred interaction behaviours of the functional groups present in LON, analysis of the Cambridge Structural Database (CSD, v 5.3.8) was completed using a number of the tools present in the software suite from the Cambridge Crystallographic Data Centre (CCDC). The methodology employed initially used Isostar, v 2.2.4[3] to find the most preferential functional groups from a pre-set list of ligands and ring systems. Next, specific contacts were investigated using the motif searching functionality in Mercury[4,5] which allowed more freedom in the description of the functional groups, a wider variety of contact groups to be searched for and a discrimination of the precise interaction occurring (exact donor and acceptor atoms in the contact). Finally, searches using the Conquest[6] search tool were undertaken to further investigate particular interactions, and different molecule fragments. Details of the models used are given in section 4.3.

4.1 Carboxylic acid

4.1.1 Isostar searches using pre-defined, general, contact groups

Uncharged Carboxylic acid-CIS 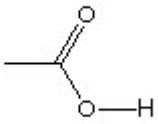	Structures have both groups present	Structures that have both groups and contact between them	%
Any polar X-H (N, O, S)	9999 (subset from 17141 structure)	2303	23.03
Alkyl CH	9999 (subset from 13315 structure)	1240	12.40
Aromatic CH	9999 (subset from 12216 structure)	1408	14.08
Any NH	7176	2100	29.26
Uncharged NH	3414	1557	45.61
Amide NH	1394	610	43.76
Uncharged C(sp^2) / C(ar)-NH2	772	531	68.78
Any OH	9999 (subset from 17141 structure)	2169	21.69
Phenol OH	1294	336	25.97
Alcohol OH	1998	1320	66.07
water	3221	1596	49.55
cyano	279	49	17.56
Any C=O	9999 (subset from 17141 structure)	2366	23.66
carboxylate	2784	1494	53.66
CONH2	553	475	85.90
Aromatic or Sp2 N	4131	1871	23.03

Uncharged Carboxylic acid- 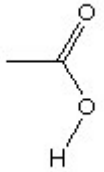 TRANS	Structures have both groups present	Structures that have both groups and contact between them	%
Any polar X-H (N, O, S)	2442	1371	56.14
Alkyl CH	1727	903	52.29
Aromatic CH	1714	1034	60.33
Any NH	1407	734	52.17
Uncharged NH	557	251	45.06
Uncharged C(sp^2) / C(ar)-NH2	67	41	61.19
Amide NH	149	88	59.06
Any OH	2442	1013	41.48
Phenol OH	101	44	43.56
Alcohol OH	212	99	46.70
water	620	430	69.35
cyano	28	5	17.86
Any C=O	2442	781	31.98
carboxylate	1007	305	30.29
CONH2	27	14	51.85
Aromatic or Sp2 N	547	112	20.48

4.1.2 Specific contact searching

				
	Carboxylic acid **OH**		Carboxylic acid **C=O**	
Contact group	No. structures	% Frequency	No. structures	% Frequency
OH	3764	13.3	10008	35.3
Ar_ hydroxy	227	11.5	1016	51.4
Al_hydroxy	1556	46.3	1633	48.6
Acyclic	2704	9.87	8505	31
Cyclic	975	23.5	1744	42
CO_2H	1810	6.89	7726	29.4
T3NH_2	521	20.7	1695	67.2
T3NH1 cyclic	409	10.1	1283	31.7
T3NH1 acyclic	222	7.25	1271	41.5
T2NH_1	14	51.9	8	29.6
T2N_any	3389	54.5		
CO**NH_2**	109	14	601	77.2
CONH_2	466	59.8		
Ar_nitrogen	2419	63.8		
Cyclic_n	601	49.8		
Acyclic_n	14	13.9		

Bold indicates the contact group used for interaction

4.1.3 Summary of CO_2H Group Results

Amide NH_2 groups appear the most favourable to form an interaction to a carboxylic acid. This is followed by any NH_2 group. Contact searching identifies aromatic nitrogen and T2N groups interacting with the OH of the carboxylic acid also to be favourable. Other favourable interactions include NH and OH, the latter having the apparent lowest propensity to form. However, when analyses are combined this low formation % observed in contact searching can be understood from the results from Isostar; phenol OH groups have a very low tendency to form, whilst alcohol OH groups have a much higher tendency. Hence, the OH value from contact searching is observed as an average and appears lower than may be expected. Detailed analysis indicates that cyclic hydroxyls are less likely to form an interaction than acyclic ones, both lower in occurrence than aliphatic and aromatic OH (aromatic > aliphatic). CO_2H groups appear to have a low tendency to form an interaction to the carboxylic acid group (interrogating just a single interaction), however further investigation using Conquest indicated that in the presence of two carboxylic acid groups, a dimer interaction is observed in 87.3% of structures. Similarly, the dimer interaction to an amide group is seen in 46.5% of structures that contain both functionalities.

Further Conquest analysis of the interaction to an aromatic or sp^2 N atom identified that almost 60% of these are neutral, with a large proportion containing charge transfer and a positive, protonated N atom. Depending on the descriptions used, approximately 42.5% contain a charged N atom. (NB, this is dependent on the charge and proton identification in the structures of the CSD). This may account for the lower than expected percentage seen in Isostar, as no information or variation on charge and protonation is possible in such searches.

4.2 Indazole

4.2.1 Isostar searches using pre-define~~d~~, general~~,~~ contact groups most relevant to the fused indazole ring in LON.

Pyrazol-1-yl	Structures have both groups present	Structures that have both groups and contact between them	%

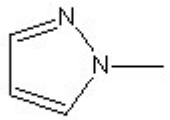			
Any polar X-H (N, S or O)`	1137	566	49.78
Alkyl CH	2368	784	33.11
Aromatic CH	2063	845	40.96
Any NH	726	256	35.26
Uncharged NH	341	88	25.81
Amide NH	186	36	19.35
Uncharged C(sp^2) / C(ar)-NH2	52	31	59.62
Any OH	561	328	58.47
Phenol OH	90	44	48.89
Alcohol OH	122	74	60.66
water	114	82	71.93
cyano	177	46	25.99
Any C=O	1099	296	26.93
carboxylate	4	1	25
CONH2	29	17	58.62
Aromatic or Sp2 N	2698	557	20.64

Pyridazine 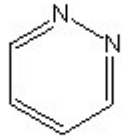	Structures have both groups present	Structures that have both groups and contact between them	%
Any polar X-H (N, O, S)	178	114	64.04
Alkyl CH	367	226	61.58
Aromatic CH	472	287	60.81
Any NH	100	58	58.00
Uncharged NH	63	28	44.44
Amide NH	17	5	29.41
Any OH	96	63	65.63
Phenol OH	32	14	43.75
Alcohol OH	8	6	75.00
water	33	22	66.67
cyano	17	8	47.06
Any C=O	130	44	33.85
carboxylate	6	3	50.00
CONH2	2	2	100.00
Aromatic or Sp2 N	510	125	24.51

4.2.2 Specific contact searching

	Pyrazoline 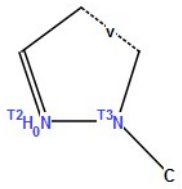		N-N 5 ring any 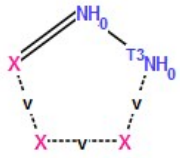		Indazole ring any 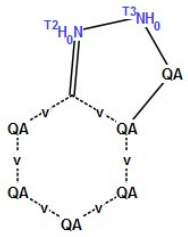		N-N=C cyclic 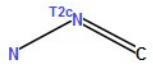		Ar_nitrogen 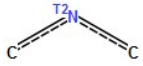	
	No. structures	% Frequency	No. structures	% Frequency	No. structures	% Frequency	No. structures	% Frequency	No. structures	% Frequency
OH	398	39	1235	28.4	7	33.3	1738	38	6276	54.8
Ar_ hydroxy	89	41.8	613	54.7	2	33.3	742	59.2	1583	52.2
Al_hydroxy	233	42.8	645	21.8	4	28.6	839	32.1	2236	45.4
Acyclic	206	42.3	458	18	4	33.3	732	28.7	3652	52.9
Cyclic	163	29.5	722	41.9	3	25	909	45.8	2072	49
CO_2H	62	40	99	16.3	0		210	26.1	2419	63.8
T3NH$_2$	178	32.3	842	28.2	2	10.5	1308	37.2	2918	49
T2NH$_1$	1	8.33	3	9.38	0		3	9.38	6	11.8
T3NH1_acyclic	102	13.1	252	9.78	1	16.7	555	17.9	2035	25.2
T3NH1_cyclic	107	19.9	347	11.6	0		1361	21.9	2117	26.8
CO**NH$_2$**	16	28.1	23	18.5	0		36	24.2	144	23
CONH$_2$	0		3	2.42	0		5	3.36	4	0.64
Methyl **CH$_3$**	167	3.99	1247	7.02	9	9.57	908	6.52	1215	5.81
Any_C-**H**	5280	86.4	24090	73	143	88.3	22343	80.8	35116	63.6
Any_**C**-H	1499	24.5	10540	32	40	24.7	9085	32.8	15810	28.6
Benzene	2	11.8	6	2.91			5	5.56	15	4.73
Methylene	2	2.82	8	2.14			8	2.84	8	1.39
Ar_C-**H**	2697	52.2	14705	57.3	82	53.9	14831	66.7	23921	44.4
Ar_C-H	772	14.9	5643	22	25	16.4	4952	22.3	10620	19.7
arCH1	772	14.9	5644	22	25	16.4	4953	22.3	10626	19.7
T3C	1059	17.8	7635	24.3	28	18.1	6792	26.3	11493	21.2
T3C-**H**	4319	72.7	16753	53.4	121	78.1	16802	65	25689	47.4
T3C-H	1061	17.9	7641	24.3	28	18.1	6797	26.3	11499	21.2
T4C	100	5.18	441	6.26	2	2.11	370	7.11	960	9.56
T4C-**H**	2508	44.1	13424	47	68	43	11592	51.3	16368	42.2
T4C-H	554	9.74	3835	13.4	14	8.86	2972	13.1	5239	13.5

Bold indicates the contact group used for interaction

4.2.3 Summary of Indazole Group Results

Analysis of the indazole group interactions was more involved, as fewer structures contain the exact fragment present in LON. A number of structurally similar fragments and functionalities were used in interaction analysis, and combined to give an overview of these groups' behaviour.

It can be seen that a general trend for the functionalities that form an interaction is C-H > OH > primary amines ($T3NH_2$) > amides > cyclic/acyclic $T3NH_1$. This can be further broken down into a

more in depth analysis of some of the groups. C-H analysis indicates T3C-H and aromatic C-H groups are the most favourable to form an interaction. Benzene, however, gives a low % frequency of interactions, indicating that the C-H groups are more likely to occur from other ring systems containing other atom types, with substitutions or with different ring sizes. T4C-H is the next most likely followed by T3C groups. Methyl groups are not very likely to form an interaction, with very low % frequency values obtained in analysis. Methylene gave similar results, with generally lower frequencies of occurrence. Therefore, for CH groups, the trend can be seen to be ar_C-H / T3C-H > T4C-H >>methyl > methylene.

OH analysis gave more variation and indicated that the results are dependent on the model used. In general, CO_2H are the least favoured OH containing functionalities to form an interaction (due to their high propensity to form a strong hydrogen bond with other strong bonding functionalities, as seen in the previous analyses). Ar_hydroxy groups feature as one of the most likely in all the models used, with frequencies of occurrence in the range 30-60%, and show a higher range of frequencies than al_hydroxy groups (20-45%). Cyclic hydroxylsappear to be slightly more favoured (25-50%) than their acyclic counterpart (18-53%) however the latter span the largest range, showing high dependence on the model used and atom environment for these interactions.

4.3 Models used for specific contact searching

General OH (T2OH$_1$) 	T3NH2 	T2N_any 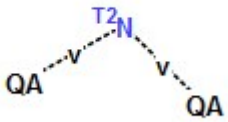	Ar_nitrogen
Ar_hydroxy 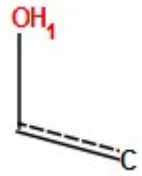	T2NH1 	Cyclic N 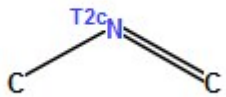	Acyclic_n 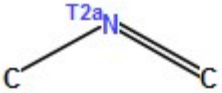

Al_hydroxy 	T3NH1 cyclic 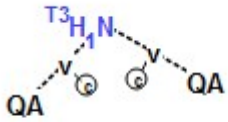	Benzene 	Methylene 
Acyclic_hydroxyl 	T3NH1 acyclic 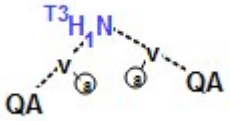	Aromatic CH1 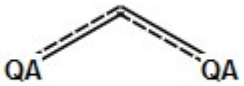	Methyl 
Cyclic_hydroxyl 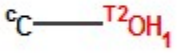	Amide 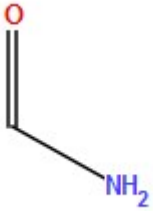	Ar_CH 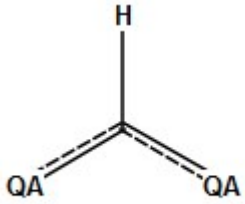	C-H 
Carboxylic acid		T3C 	T3C-H 
		T4C 	T4C-H 

QA denotes any atom except hydrogen, c=cyclic, a=acyclic, TX=no. of bonded atoms (eg T2 = 2 bonded atoms to atom indicated), dashed bonds indicate any bond type (not specified).

5. Co-formers Used in Screening Experiments

Bold text indicates successful co-crystal / salt formation and a new material produced

2,2'-Di-n-propylacetamide (Valpromide)
2,4,6-Triaminopyrimidine
2,5-pyridinedicarboxylic acid
2-Amino-5-bromobenzoic acid
2-Amino-5-bromopyrimidine
2-Aminopyridine
2-Aminopyrimidine
2-Ethoxybenzamide
2-Picolinic acid
3,5-Dihydroxybenzoic acid
3-Aminobenzoic acid
3-Ethynylpyridine
3-Nitrobenzamide
4,4'-Bipyridine
4,5-Dichlorophthalic acid
4-Aminobenzamide
4-Dimethylaminopyridine
4-Hydroxybenzamide
4-Hydroxybenzoic acid
5-Aminosalicylic acid
5-Fluorouracil
Acesulfame
Acetazolamide
Adenine
Adipamide
Aspartame
Aspirin
Benzamide
Benzoin
Camphoric acid
Caprolactam
Catechol
Chlorhexidine
Chlorpropamide
Cytosine
D-Methionine
Flufenamic acid
Gallic acid
Haloperidol
Hydroxyurea
Ibuprofen
Imidazole
Indole-3-acetic acid
Isoniazid
Isonicotinamide
Isonicotinic acid
Isophthalic acid
L-Alanine
L-Arginine
L-Glutamine
L-Threonine
Melamine
Myo-inositol
Nalidixic acid
Nicotinamide
Nicotinic acid
Orotic acid
Oxalic acid
p-Coumaric acid
Phloroglucinol
Picolinamide
Piperazine
Piperine
Piracetam
Propionamide
Pyrazineamide
Pyridoxine
Pyrogallol
Quinoxaline
Resorcinol
Rufinamide
Saccharin
Salbutamol
Salicylamide
Salicylic acid
Sarcosine
Sulfamethoxypyridazine
Sulfamic acid
Taurine
Terephthalic acid

Theophylline
Thymine
Trans-3-hydroxycinnamic acid
Uracil
Urea
Vanillic acid
γ-Glycine

6. PXRD Patterns – screening by solid-state grinding

6.1. Successful grinding samples – pharmaceutical co-formers

Grinding samples which resulted in new materials containing pharmaceutically acceptable co-formers and for which a crystal structure was determined (Figures 8-14).

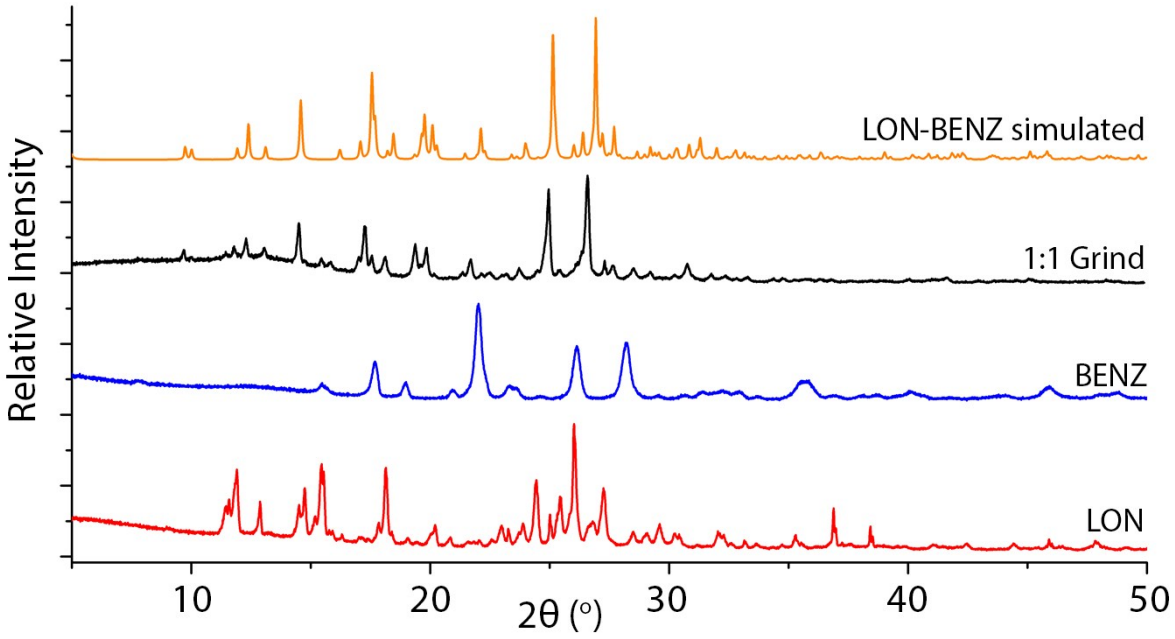

Figure 8. PXRD for 1:1 solvent drop grind of LON with BENZ compared to the simulated pattern from the crystal structure obtained.

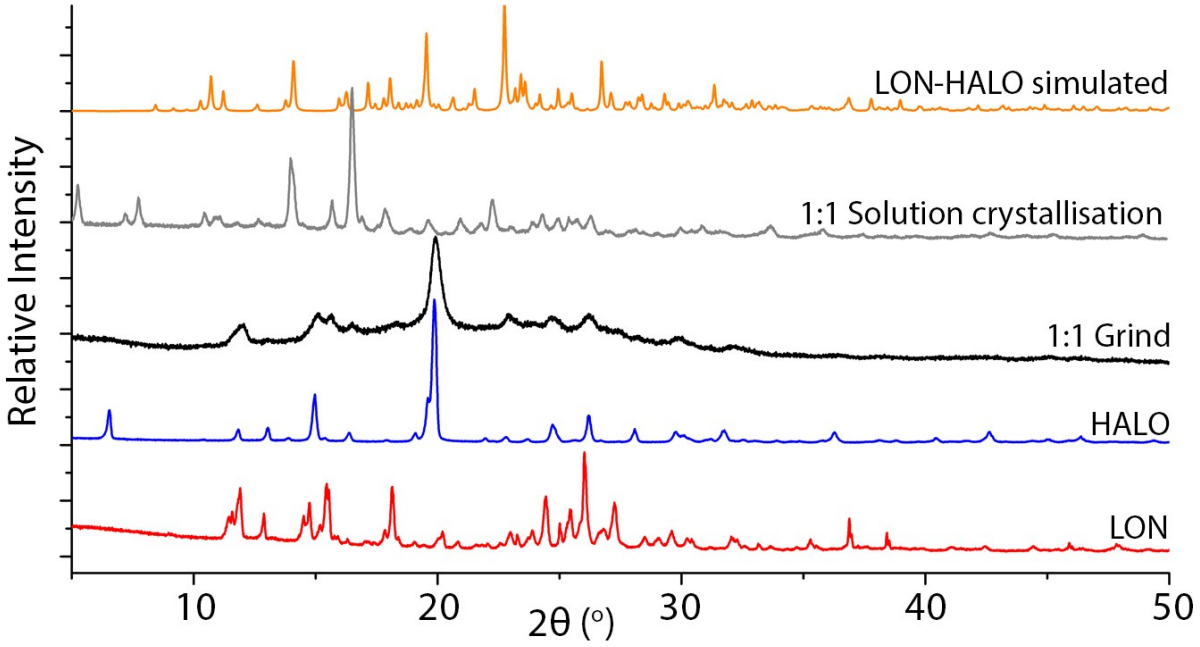

Figure 9. PXRD for 1:1 solvent drop grind and powder produced from solution experiment (salt formed) of LON with HALO compared to the simulated pattern from the crystal structure obtained. Grinding methods did not produce the material identified by SCXRD.

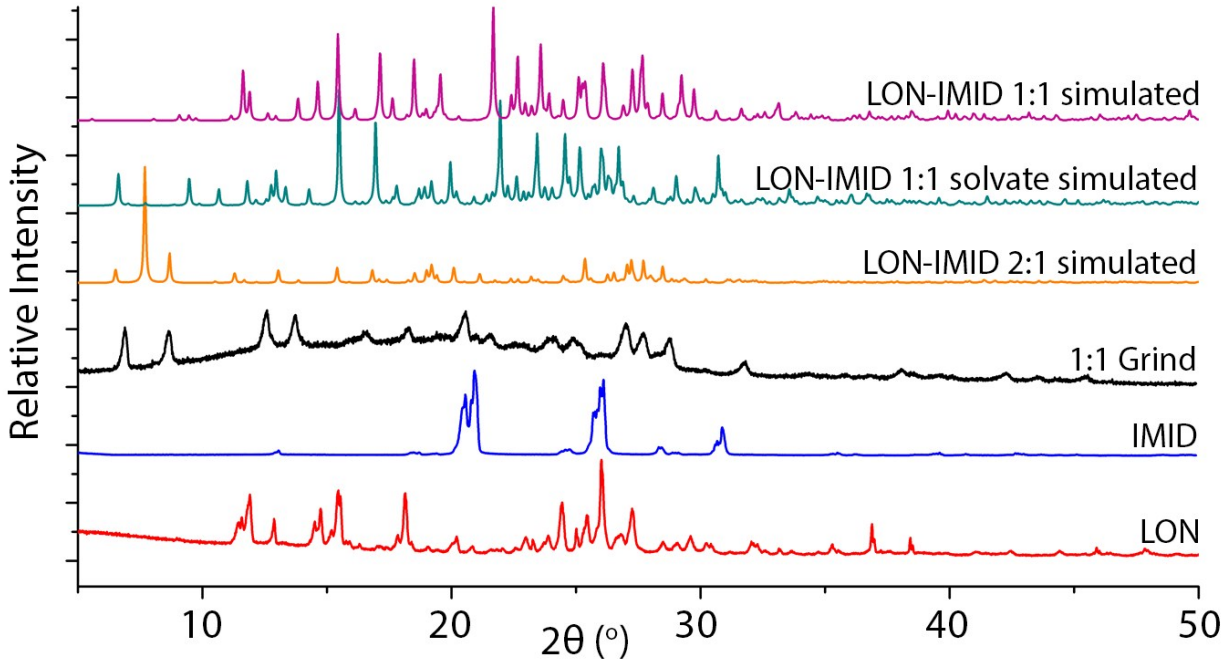

Figure 10. PXRD for 1:1 solvent drop grind of LON with IMID compared to the simulated patterns from all three crystal structures obtained. Material was poorly crystalline however shows likeness to the 2:1 structure.

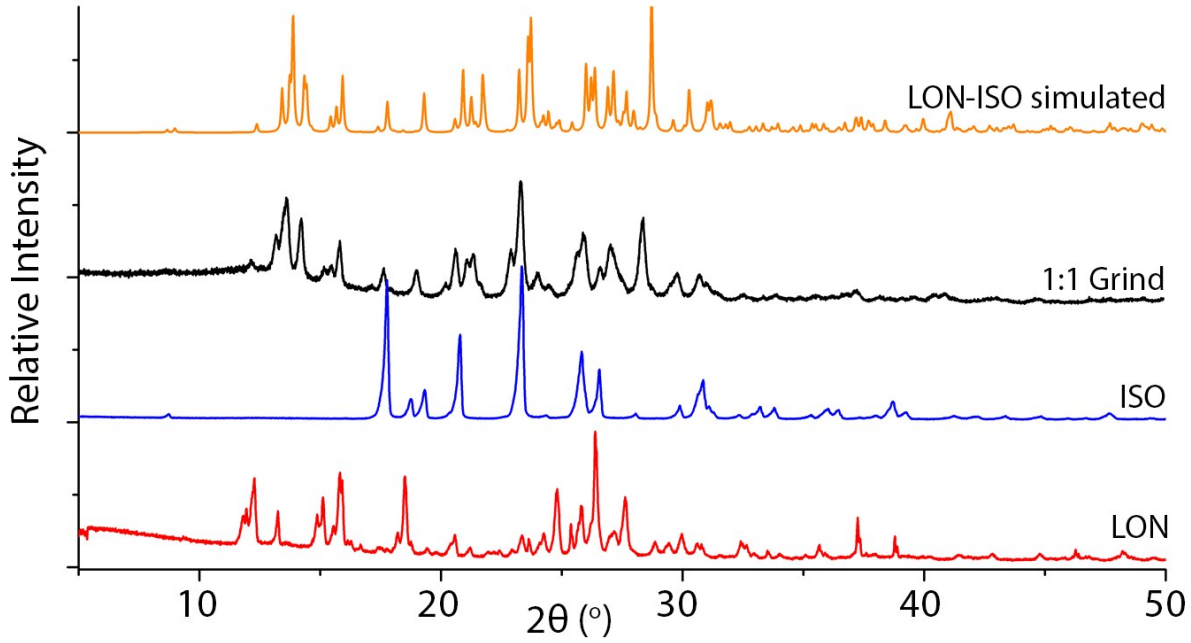

Figure 11. PXRD pattern for 1:1 solvent drop grind of LON with ISO compared to the simulated pattern from the crystal structure obtained.

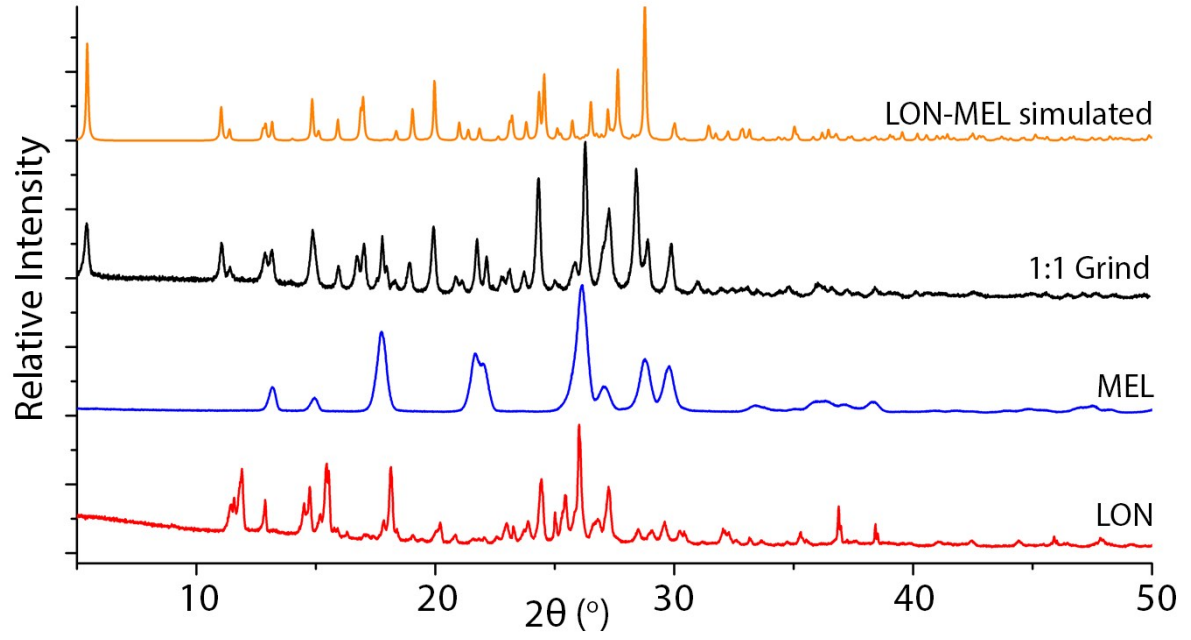

Figure 12. PXRD for 1:1 solvent drop grind of LON with MEL compared to the simulated pattern from the crystal structure obtained.

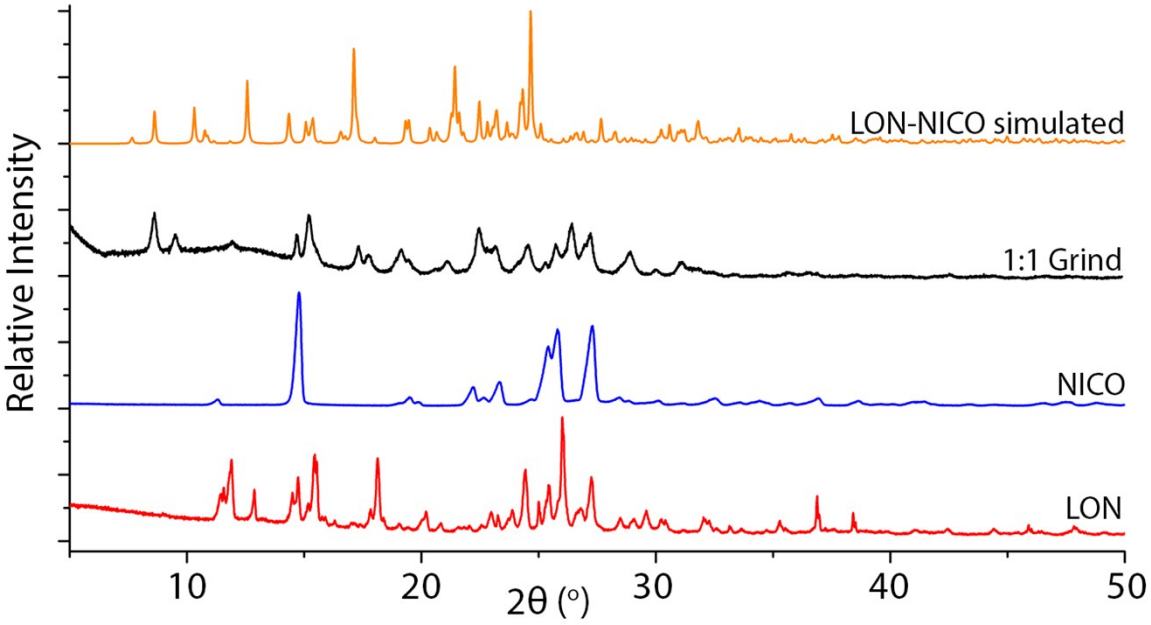

Figure 13. PXRD for 1:1 solvent drop grind of LON with NICO compared to the simulated pattern from the crystal structure obtained.

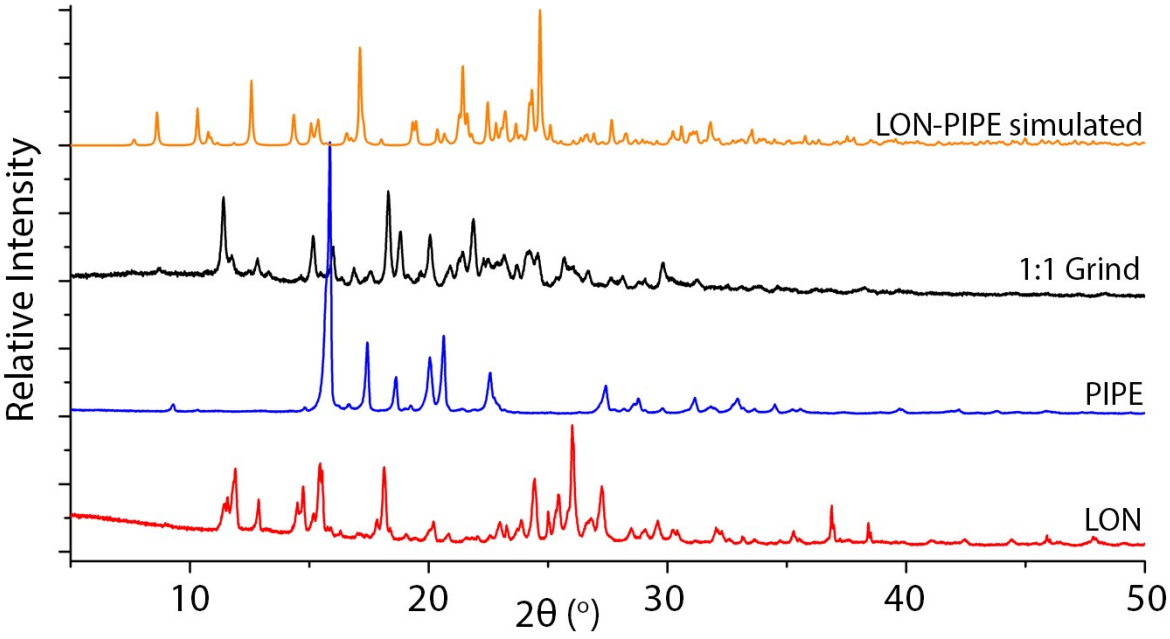

Figure 14. PXRD for 1:1 solvent drop grind of LON with PIPE compared to the simulated pattern from the crystal structure obtained. Grinding indicated poor conversion into the salt form with some parent material still present.

6.2. Successful grinding samples – non pharmaceutical co-formers

In addition to the reported novel materials containing pharmaceutically acceptable co-formers, a number of materials were also generated with five other co-formers (from screening) that are not pharmaceutically acceptable:

- 2-Aminopyridine, 2APYD
- 2-Aminopyrimidine, 2APYM
- 4-Dimethylaminopyridine, 4DMAP
- 2,4,6-Triaminopyrimidine, 246TAPYM
- 4,4'-Bipyridine, 4,4BIPY

PXRD patterns from screening by grinding are displayed in Figures 15-19 and crystals structures were determined for all.

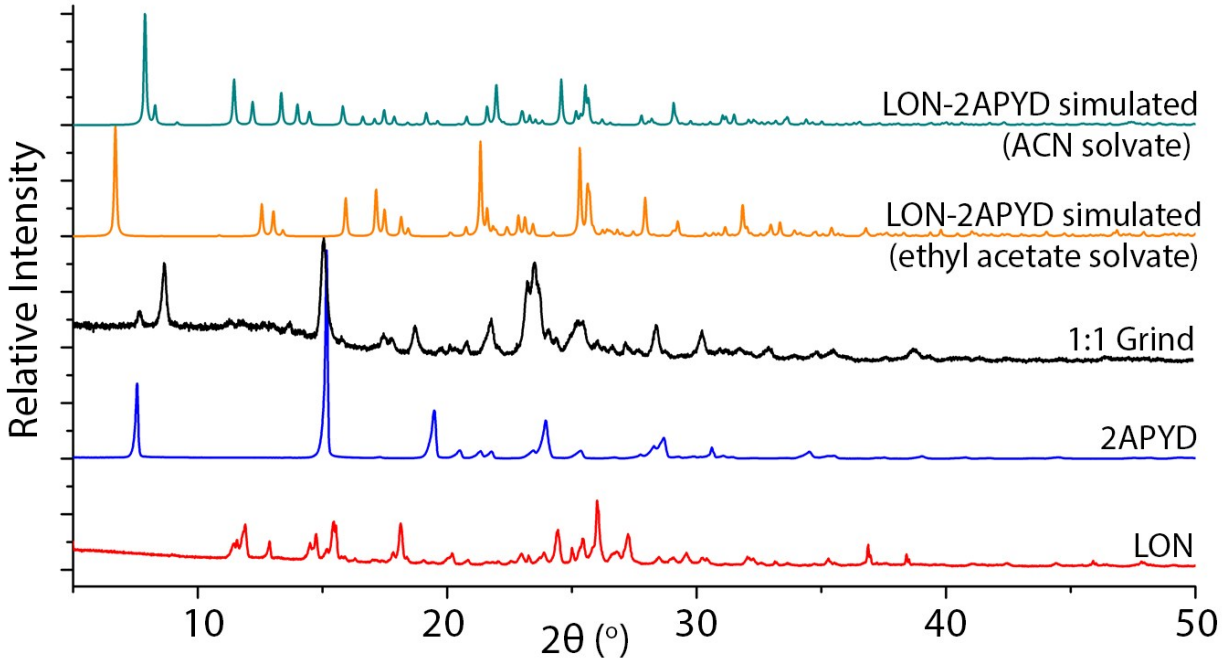

Figure 15. PXRD for 1:1 solvent drop grind of LON with 2APYD compared to the simulated patterns from the crystal structures obtained.

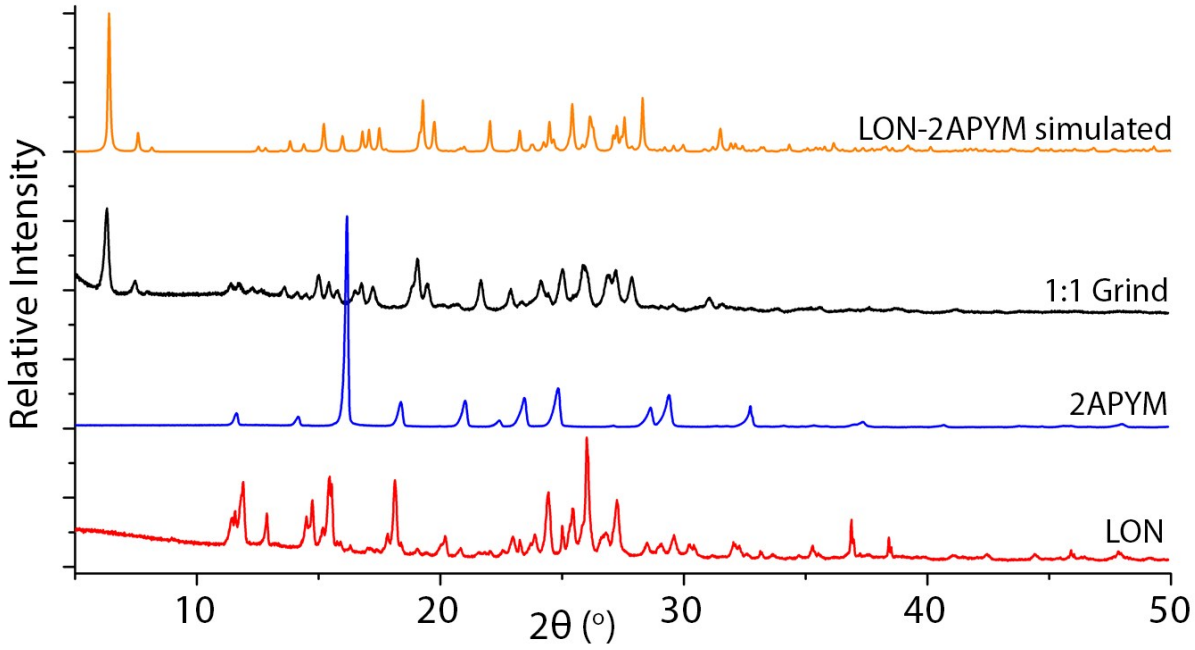

Figure 16. PXRD for 1:1 solvent drop grind of LON with 2APYM compared to the simulated pattern from the crystal structure obtained.

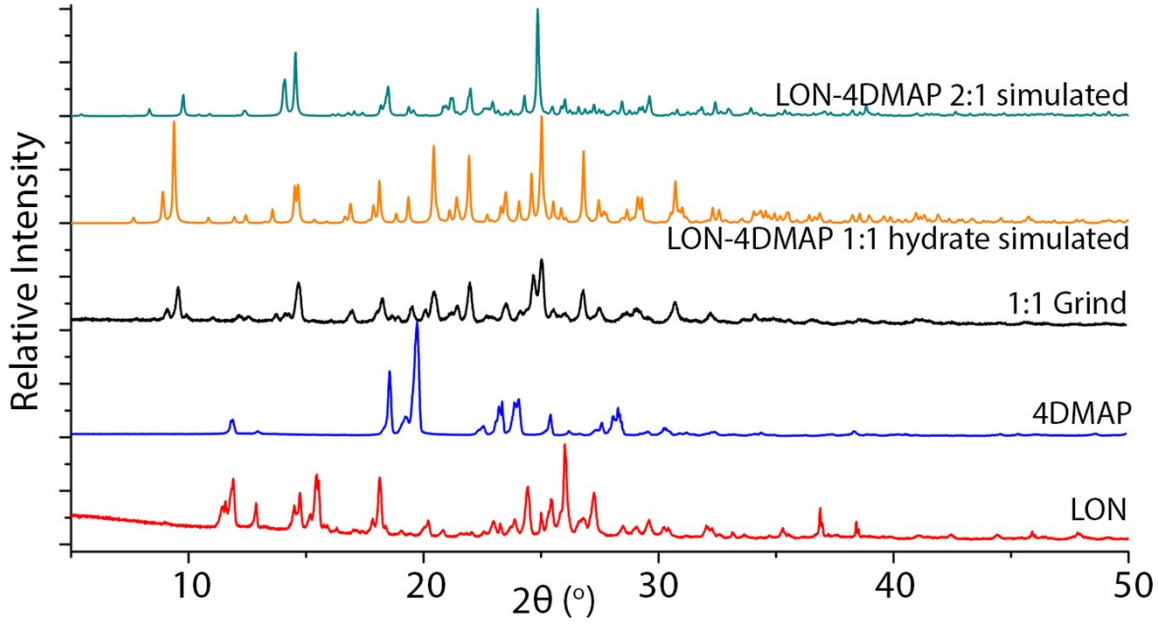

Figure 17. PXRD for 1:1 solvent drop grind of LON with 4DMAP compared to the simulated patterns from the crystal structures obtained.

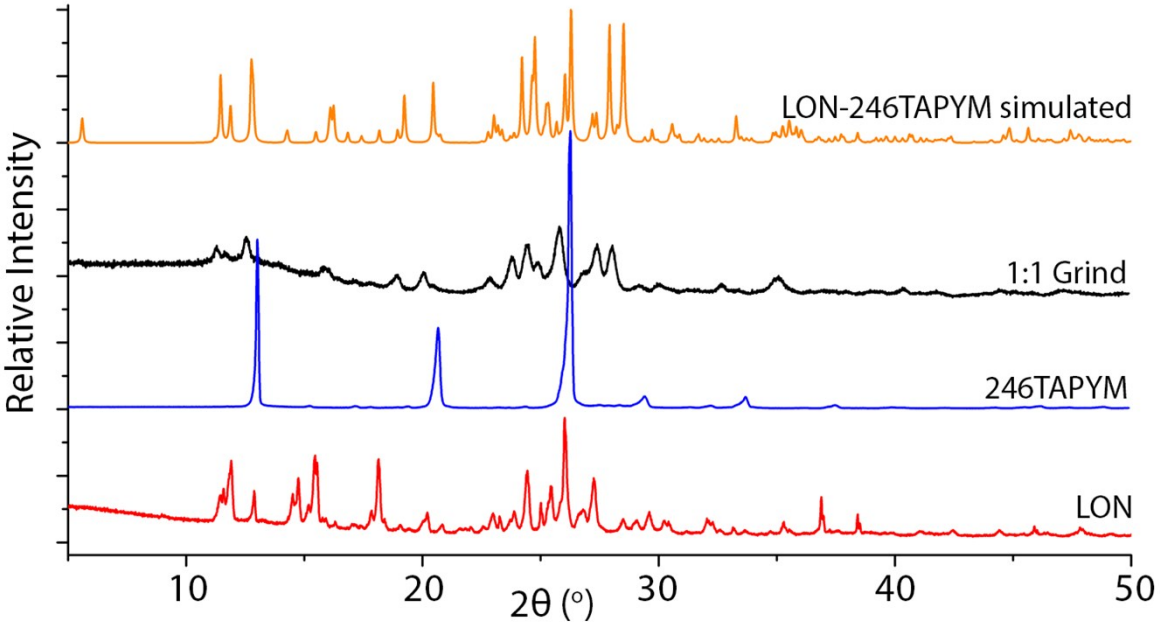

Figure 18. PXRD for 1:1 solvent drop grind of LON with 246TAPYM compared to the simulated pattern from the crystal structure obtained.

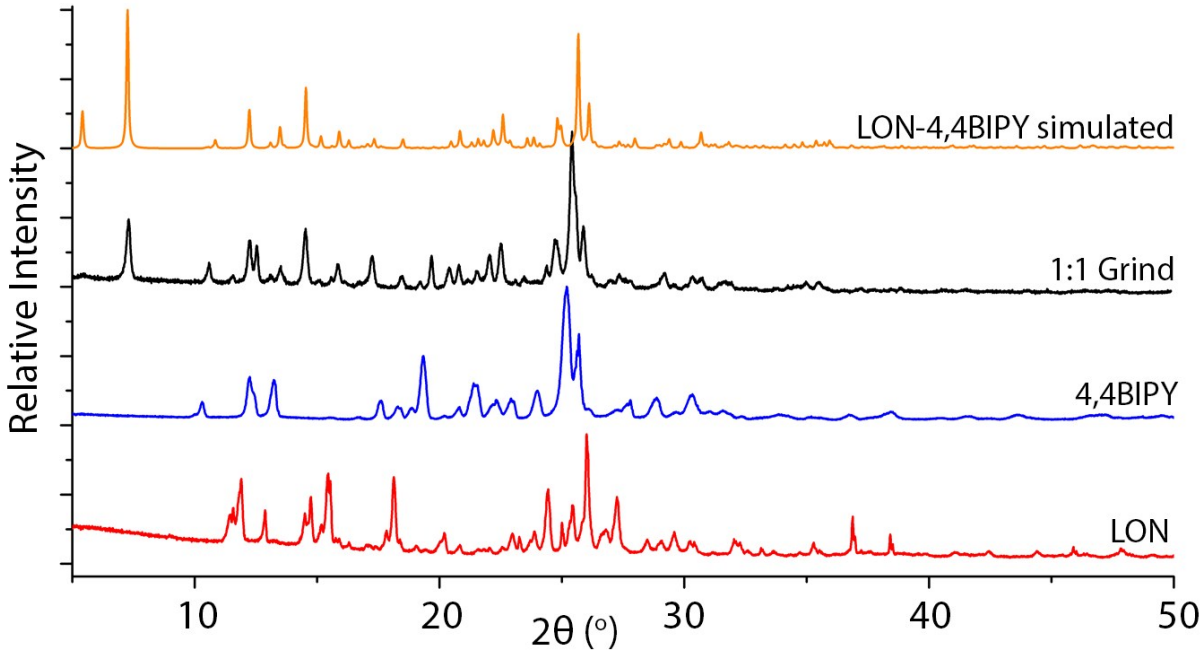

Figure 19. PXRD for 1:1 solvent drop grind of LON with 4,4BIPY compared to the simulated pattern from the crystal structure obtained.

6.3. Potential from grinding

Solvent drop grinding experiments with the following co-formers (Figure 20) indicated potential for a new form, however no crystals were produced to allow structure determination by single crystal X-ray diffraction:

- 3-Ethynylpyridine
- 4-Hydroxybenzamide
- 4,5-Dichlorophthalic acid
- Aspartame
- Pyridoxine
- Quinoxaline
- Theophylline

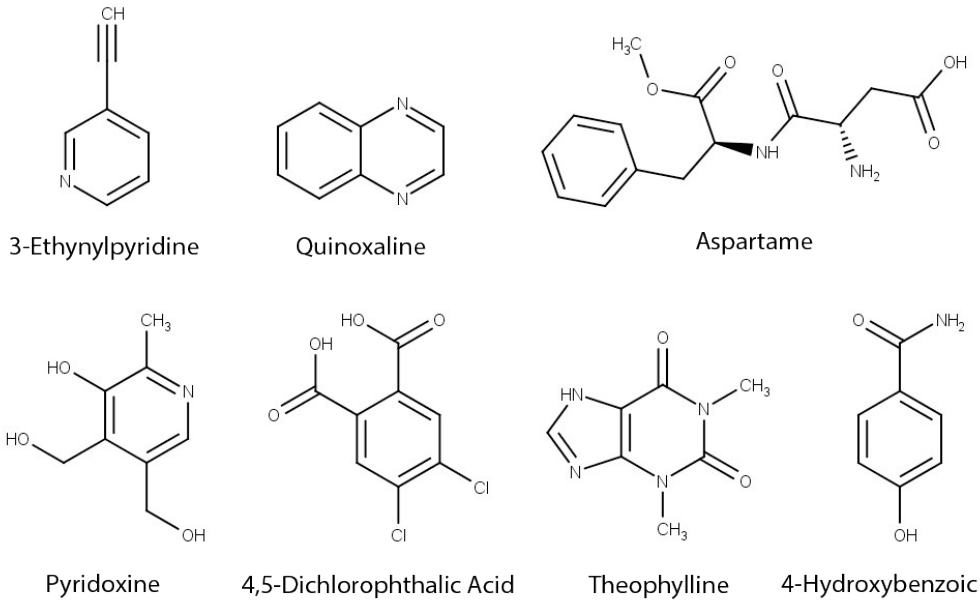

Figure 20. Structure of co-formers which indicated potential from grinding experiments however no single crystals were produced for diffraction experiments.

Figures 21-27 show the PXRD pattern for the material obtained from grinding compared to the parent material reference patterns and the two polymorphs of LON. This enables the new peaks observed to be identified as indicative of a new form and not due to polymorphic conversion.

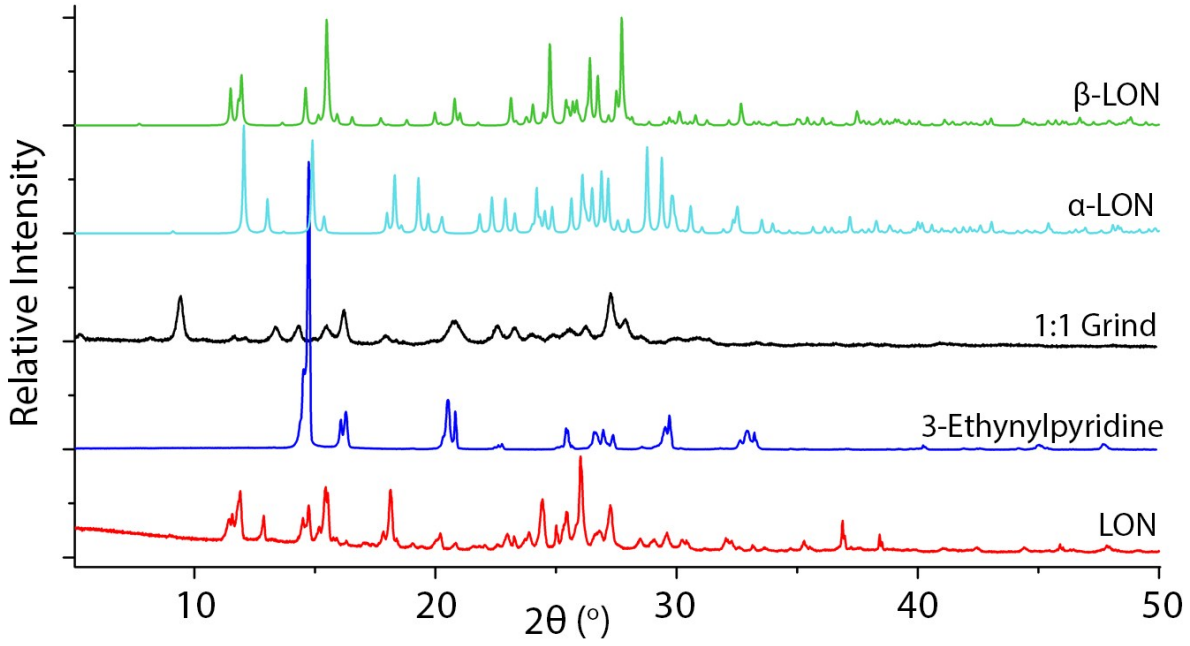

Figure 21. PXRD for 1:1 solvent drop grind of LON with 3-ethynylpyridine.

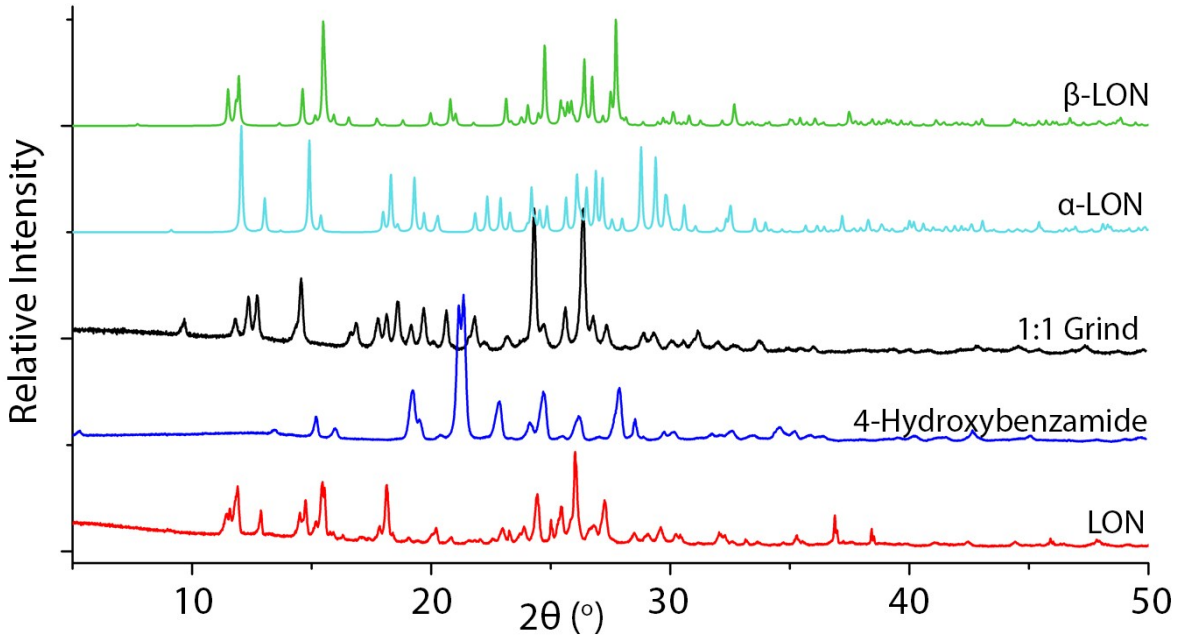

Figure 22. PXRD for 1:1 solvent drop grind of LON with 4-hydroxybenzamide.

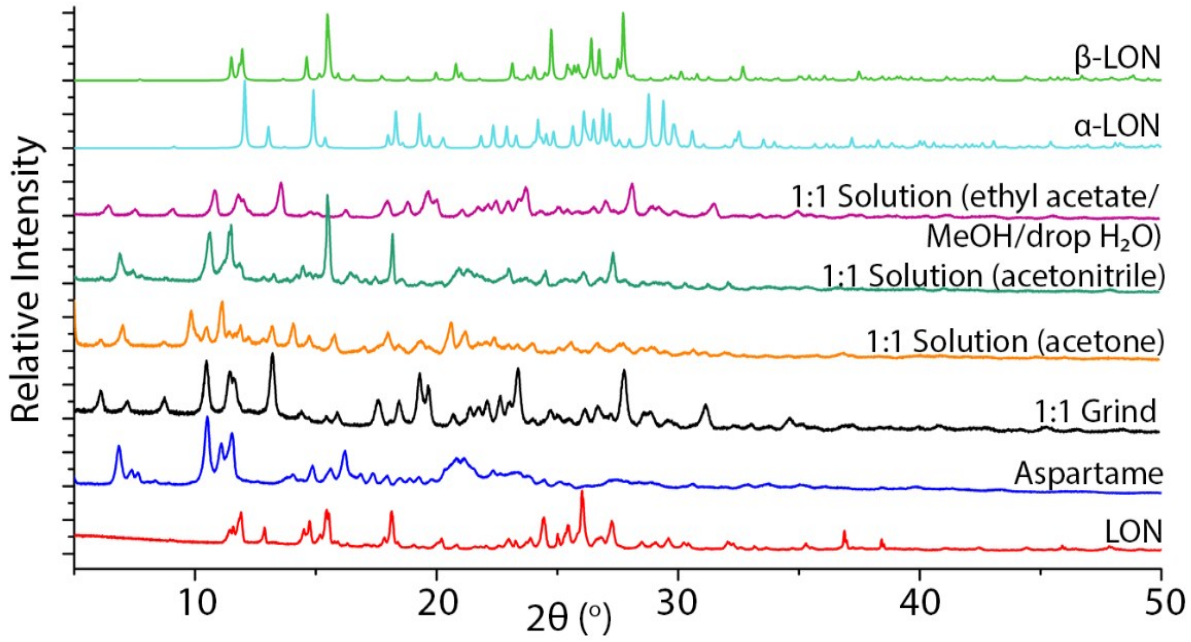

Figure 23. PXRD for 1:1 solvent drop grind and various solution attempts (powders) of LON with aspartame.

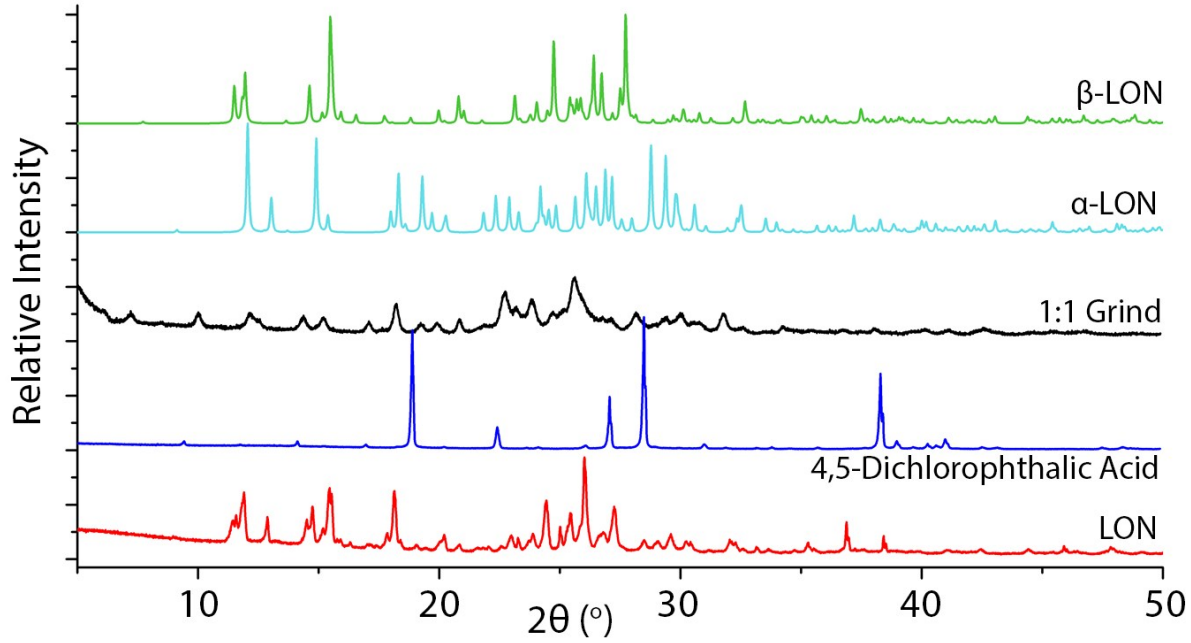

Figure 24. PXRD for 1:1 solvent drop grind of LON with 4,5-dichlorophthalic acid.

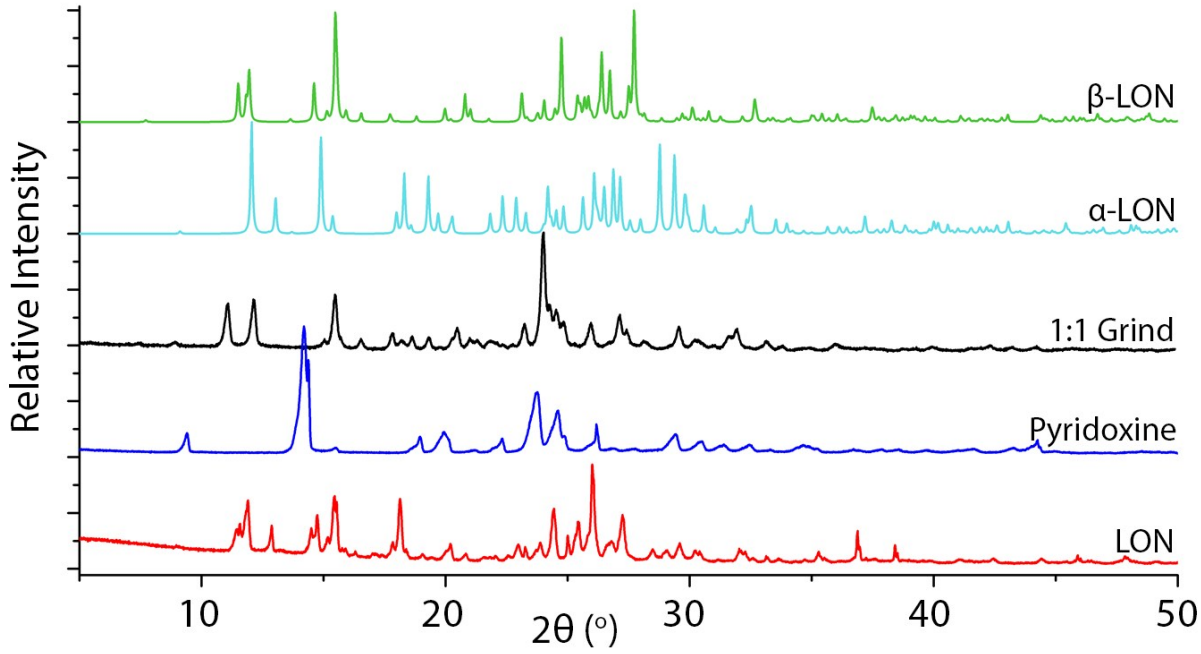

Figure 25. PXRD for 1:1 solvent drop grind of LON with pyridoxine.

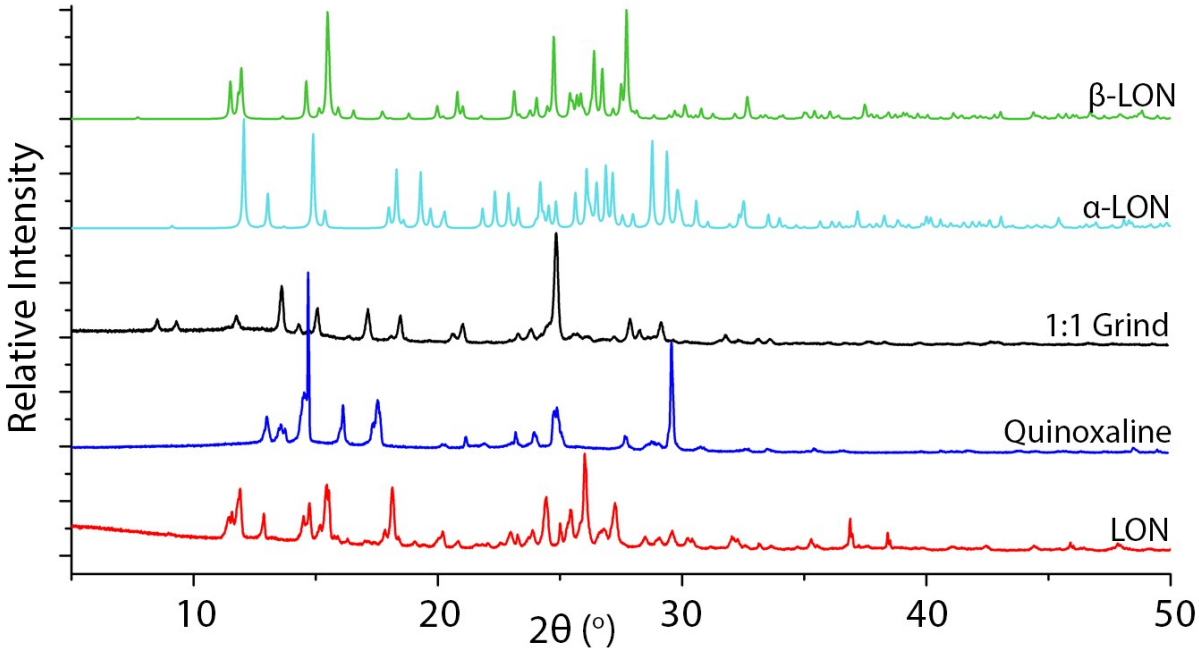

Figure 26. PXRD for 1:1 solvent drop grind of LON with quinoxaline.

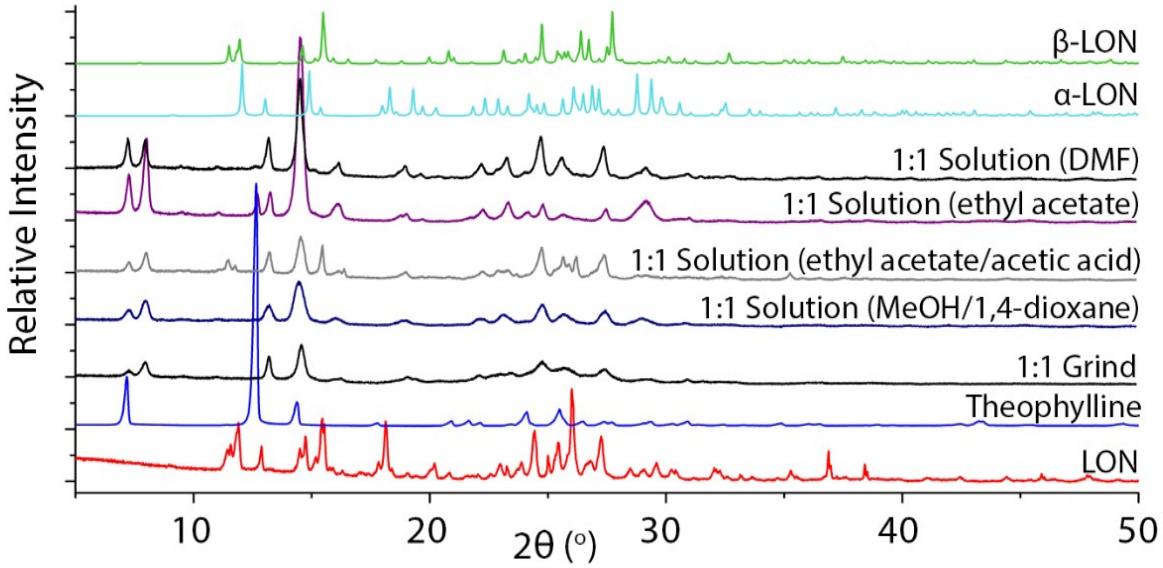

Figure 27. PXRD for 1:1 solvent drop grind and solution attempts of LON with theophylline.

7. Crystal Structures

7.1. Parameters for crystal structures reported in this paper

Table 7.1.1. Crystal structure parameters for two polymorphs of LON and crystal structures containing pharmaceutically acceptable co-formers.

Compound Reference	**α-LON**	**β-LON**	**LON-BENZ 1:1**	**LON-HALO 1:1 trihydrate**	**LON-IMID 1:1:0.5 ethyl acetate solvate**	**LON-IMID 2:1**	**LON-IMID 1:1**
Crystal Data							
Chemical Formula	$C_{15}H_{10}Cl_2N_2O_2$	$C_{15}H_{10}Cl_2N_2O_2$	$C_{15}H_{10}Cl_2N_2O_2 \cdot C_7H_7N_1O_1$	$C_{15}H_9Cl_2N_2O_2 \cdot C_{21}H_{24}ClFNO_2 \cdot 3(H_2O)$	$C_{15}H_9Cl_2N_2O_2 \cdot C_3H_5N_2 \cdot 0.5(C_4H_8O_2)$	$2(C_{15}H_{9.5}Cl_2N_2O_2) \cdot C_3H_5N_2$ [a]	$C_{15}H_{9.5}Cl_2N_2O_2 \cdot C_{15}H_9Cl_2N_2O_2 \cdot C_3H_5N_2 \cdot C_3H_{4.5}N_2$
*M*r	321.15	321.15	442.28	751.05	433.28	710.38 [a]	778.46
Density /gcm^{-1}	1.586	1.539	1.454	1.410	1.426	1.415	1.475
Crystal size /mm	0.326 x 0.028 x 0.012	0.384 x 0.204 x 0.116	0.05 x 0.05 x 0.01	0.282 x 0.146 x 0.031	0.393 x 0.22 x 0.145	0.679 x 0.378 x 0.224	0.05 x 0.05 x 0.01
Crystal colour, morphology	Colourless, needle	Colourless, block	Colourless, plate	Colourless, plate	Colourless, block	Colourless, block	Colourless, chip
Crystal system	Monoclinic	Triclinic	Monoclinic	Monoclinic	Monoclinic	Triclinic	Triclinic
Space group	$P2_1/c$	$P\bar{1}$	$P21/c$	$I2/a$	$P2_1/c$	$P\bar{1}$	$P\bar{1}$
a/Å	19.3743(10)	7.5759(3)	18.3534(8)	16.8612(5)	15.1394(5)	10.3787(7)	10.0605(5)
b/Å	4.7313(2)	8.0832(3)	10.1000(3)	10.8847(3)	29.9418(9)	11.8719(9)	11.0252(6)
c/Å	14.6770(7)	11.9077(4)	11.0376(4)	39.3807(11)	26.9456(6)	14.0409(8)	16.3298(10)
α/°	90.00	105.626(3)	90.00	90.00	90.00	105.139(6)	88.224(5)
β/°	91.886(4)	91.790(3)	99.146(4)	101.781(3)	97.628(2)	91.651(5)	76.212(5)
γ/°	90.00	98.360(3)	90.00	90.00	90.00	91.906(6)	84.969(4)
Cell volume / Å^3	1344.65(11)	692.88(5)	2020.02(13)	7075.3(3)	12106.4(6)	1667.8(2)	1752.21(17)
Z	4	2	4	8	24	2	2

Data Collection

Diffractometer	Agilent Technologies, Dual Source Supernova	Agilent Technologies, Dual Source Supernova	Rigaku FRE+	Agilent Technologies, Dual Source Supernova	Agilent Technologies, Dual Source Supernova	Agilent Technologies, Dual Source Supernova	Rigaku FRE+
Temperature /K	100	100	100	100	100	100	100
Radiation Type	Mo K\α	Mo K\α	Mo K\a	Mo K\α	Mo K\α	Mo K\α	Mo K\α
Wavelength, λ /Å	0.71073	0.71073	0.71075	0.71073	0.71073	0.71073	0.71075
R_{int}	0.0636	0.0208	0.0421	0.0288	0.0383	*	0.0464
No. of reflections measured	9905	9562	33938	25559	86240	40327	21522
No. of unique reflections	3074	3183	4631	8099	27727	12547	8029
Completeness /%	99.71	99.97	99.98	99.85	99.81	99.83	99.90

Refinement

GoF, S	1.110	1.044	1.024	1.024	1.030	1.076	1.039
Final R_1 ($I > 2\sigma(I)$)	0. 0600	0.0281	0.0424	0.0478	0.0628	0.0717	0.0553
Final R_1 (all data)	0.0842	0.0306	0.0558	0.0634	0.0876	0.0830	0.0833
Final w$R(F^2)$ ($I > 2\sigma(I)$)	0.1318	0.0720	0.1068	0.1043	0.1575	0.2024	0.1378
Final w$R(F^2)$ (all data)	0.1439	0.0737	0.1143	0.1109	0.1737	0.2092	0.1521

Compound Reference	**LON-ISO 1:1**	**LON-MEL 1:1**	**LON-NICO 1:1**	**LON-PIPE 2:1**
Chemical Formula	$C_{15}H_{10}Cl_2N_2O_2 \cdot C_6H_6N_2O_1$	$C_{15}H_9Cl_2N_2O_2 \cdot C_3H_7N_6$	$C_{15}H_{10}Cl_2N_2O_2 \cdot C_6H_6N_2O_1$	$2(C_{15}H_9Cl_2N_2O_2) \cdot C_4H_{12}N_2$
*M*r	443.28	447.29	443.28	728.44
Density /gcm^{-1}	1.502	1.584	1.534	1.445
Crystal size /mm	0.459 x 0.359 x 0.188	1.0 x 0.121 x 0.057	0.28 x 0.03 x 0.01	0.784 x 0.109 x 0.069
Crystal colour, morphology	Colourless, block	Colourless, needle	Colourless, plate	Colourless, block
Crystal system	Monoclinic	Triclinic	Monoclinic	Triclinic
Space group	$P2_1/n$	$P\bar{1}$	$P2_1/c$	$P\bar{1}$
a/Å	12.9910(3)	7.0752(4)	20.6918(6)	11.6186(5)
b/Å	7.6724(2)	8.1750(4)	4.61421(12)	12.3390(8)
c/Å	19.8344(5)	16.8057(10)	20.1099(5)	12.5559(7)
α/°	90.00	99.416(5)	90.00	68.926(6)
β/°	97.409(2)	100.168(5)	90.673(2)	85.447(4)
γ/°	90.00	94.778(5)	90.00	88.975(4)
Cell volume / Å^3	1960.43(9)	937.57(9)	1919.89(9)	1674.24(17)
Z	4	2	4	2
Data Collection				
Diffractometer	Agilent technologies, Dual Source Supernova	Agilent technologies, Dual Source Supernova	Rigaku FRE+	Agilent Technologies, Dual Source Supernova
Temperature /K	100	100	100	100
Radiation Type	Mo K\α	Mo K\α	Mo K\α	Mo K\a

Wavelength, λ /Å	0.71073	0.71073	0.71075	0.71073
R_{int}	0.0456	0.0320	0.0495	*
No. of reflections measured	34896	13981	36705	36628
No. of unique reflections	4486	4299	4368	13510
Completeness /%	99.88	99.95	99.92	99.90
Refinement				
GoF, S	1.048	1.041	1.069	1.047
Final R_1 ($I > 2\sigma(I)$)	0.0393	0.0360	0.0532	0.0511
Final R_1 (all data)	0.0453	0.0406	0.0578	0.0622
Final w$R(F^2)$ ($I > 2\sigma(I)$)	0.0926	0.0892	0.1515	0.1540
Final w$R(F^2)$ (all data)	0.0967	0.0921	0.1569	0.1582

* Non-merohedral twin, all data are merged

[a] LON-IMID 2:1 contains voids which may contain solvent (MeOH / acetonitrile or water molecules)

Table 7.1.2. Crystal structure parameters for crystal structures containing non-pharmaceutically acceptable co-formers.

Compound Reference	**LON-2APD 1:1 ACN solvate**	**LON-2APD 1:1:1 ethyl acetate solvate**	**LON-2AYPM 2:1**	**LON-246TAPYM 1:1**	**LON-4DMAP 2:1**	**LON-4DMAP 1:1 dihydrate**	**LON-4,4BIPY 2:1**
Chemical Formula	C_{15} H_9 Cl_2 N_2 O_2 · C_5 H_7 N_2	C_{15} H_9 Cl_2 N_2 O_2 · C_5 H_7 N_2 · C_4 H_8 O_2	C_{15} H_{10} Cl_2 N_2 O_2 · 2(C_4 H_5 N_3)	C_{15} H_9 Cl_2 N_2 O_2 · C_4 H_8 N_5	C_{15} H_{10} Cl_2 N_2 O_2 · C_{15} H_9 Cl_2 N_2 O_2 · C_7 H_{11} N_2	C_{15} H_9 Cl_2 N_2 O_2 · C_7 H_{11} N_2 · 2(H_2 O)	2(C_{15} H_{10} Cl_2 N_2 O_2)· C_{10} H_8 N_2
*M*r	415.27 (excluding solvent)	503.37	511.37	446.29	764.47	479.35	798.48
Density /gcm^{-1}	1.347	1.389	1.486	1.575	1.483	1.435	1.428
Crystal size /mm	0.772 x 0.092 x 0.016	1.0 x 0.156 x 0.129	0.282 x 0.147 x 0.066	0.261 x 0.201 x 0.138	0.27 x 0.089 x 0.053	0.898 x 0.122 x 0.11	0.04 x 0.03 x 0.01
Crystal colour, morphology	Colourless, plate	Colourless, block	Colourless, plate	Colourless, prism	Colourless, plate	Colourless, block	Colourless, plate
Crystal system	Monoclinic	Monoclinic	Monoclinic	Monoclinic	Triclinic	Monoclinic	Monoclinic
Space group	$P2_1/c$	Pc	$P2_1/c$	$P2_1/n$	$P\bar{1}$	$P2_1/c$	$P2_1/c$
a/Å	11.1266(5)	10.9724(3)	14.1417(6)	7.7720(12)	8.5711(2)	13.0507(6)	32.6725(11)
b/Å	22.3945(10)	13.1874(3)	21.6532(8)	31.5262(14)	12.3681(4)	9.03300(18)	26.2388(13)
c/Å	8.5821(5)	8.8415(3)	7.6525(3)	11.6214(18)	16.6270(5)	24.7738(11)	8.6827(3)
α/°	90.00	90.00	90.00	90.00	79.963(3)	90.00	90.00
β/°	106.718(6)	109.768(3)	102.654(4)	138.80(3)	81.329(2)	130.546(8)	93.879(3)
γ/°	90.00	90.00	90.00	90.00	84.947(3)	90.00	90.00
Cell volume / Å^3	2048.06(19)	1203.95	2286.39(16)	1875.4(8)	1712.33(9)	2219.3(2)	7426.6(5)
Z	4	2	4	4	2	4	8

Data Collection							
Diffractometer	Agilent technologies, Dual Source Supernova	Agilent technologies, Dual Source Supernova	Agilent technologies, Dual Source Supernova	Agilent technologies, Dual Source Supernova	Agilent technologies, Dual Source Supernova	Agilent technologies, Dual Source Supernova	Rigaku FRE+
Temperature /K	100	100	100	100	100	100	100
Radiation Type	Mo K\α	Mo K\α	Mo K\α	Mo K\α	Mo K\α	Mo K\α	Mo K\α
Wavelength /λ	0.71073	0.71073	0.71073	0.71073	0.71073	0.71073	0.71075
R_{int}	0.0330	0.0211	0.0705	0.0278	0.0363	0.0238	0.0669
No. of reflections measured	14679	9655	27846	29914	24011	19704	50025
No. of unique reflections	4674	4992	5218	4304	7913	5078	17020
Completeness /%	99.36	99.90	99.91	99.90	99.97	99.96	99.87
Refinement							
GoF, S	1.033	1.051	1.138	1.185	1.048	1.058	0.974
Final R_1 ($I > 2\sigma(I)$)	0.0499	0.0322	0.0582	0.0419	0.0466	0.0322	0.0758
Final R_1 (all data)	0.0692	0.0335	0.0815	0.0424	0.0611	0.0357	0.1561
Final w$R(F^2)$ ($I > 2\sigma(I)$)	0.1045	0.0820	0.1054	0.0965	0.0994	0.0822	0.1516
Final w$R(F^2)$ (all data)	0.1105	0.0830	0.1130	0.0967	0.1056	0.0846	0.1740

7.2. Neutron normalised intermolecular interactions in the crystal structures of the salts/co-crystals of LON

Table 6.2.1. Interactions for crystal structures containing pharmaceutically acceptable co-formers

Sample	D–H···A*	H···A /Å	D···A /Å	D–H···A /°	Symmetry code
α-LON	O(1)-H(1)···O(2)	1.67	2.648(3)	174	1-*x*, -*y*, 1-*z*
	C(5)-H(5)···O(2)	2.44	3.387(4)	146	1-*x*, ½+*y*, ½-*z*
***β*-LON**	O(1)-H(1)···O(2)	1.64	2.6232(13)	175	2-*x*, 1-*y*, 2-*z*
	C(12)-H(12)···O(1)	2.46	3.5464(16)	178	1-*x*, 1-*y*, 1-*z*
	C(12)-H(12)···N(2)	2.56	3.1764(16)	115	1-*x*, 1-*y*, 1-*z*
LON-BENZ	O(1)-H(1)···O(21)	1.57	2.5480(17)	172	
	N(21)-H(21A)···O(2)	1.88	2.877(2)	169	
	N(21)-H(21B)···O(1)	2.51	3.113(2)	118	*x*, ½-*y*, ½+*z*
	N(21)-H(21B)···N(2)	2.19	3.107(2)	151	*x*, ½-*y*, ½+*z*
	C(6)-H(6)···O(2)	2.38	3.218(2)	133	1-*x*, ½+*y*, 3/2-*z*
	C(12)-H(12)···O(21)	2.37	3.382(2)	154	*x*, 1+*y*, *z*
	C(25)-H(25)···Cl(2)	2.70	3.728(2)	159	2-*x*, -3/2+*y*, 3/2-*z*
LON-HALO trihydrate	N(21)-H(21)···O(2)	1.72	2.724(2)	172	
	O(22)-H(22)···O(41)	1.78	2.727(3)	160	
	O(41)-H(41A)···O(2)	1.76	2.737(3)	175	½+*x*, 1-*y*, *z*
	O(41)-H(41B)···O(1)	1.76	2.727(3)	169	1-*x*, -½+*y*, ½-*z*
	O(42)-H(42A)···O(43)	1.91	2.831(10)	154	
	O(42)-H(42B)···O(21)	2.01	2.976(7)	166	1-*x*, ½+*y*, ½-*z*
	O(43)-H(43A)···O(42)	1.82	2.790(8)	169	3/2-*x*, 3/2-*y*, ½-*z*
	O(43)-H(43B)···O(1)	2.02	2.873(6)	143	1-*x*, -½+*y*, ½-*z*
	C(7)-H(7)···Cl(1)	2.70	3.709(2)	155	
	C(9)-H(9B)···Cl(1)	2.55	3.131(2)	113	
	C(30)-H(30A)···O(21)	2.52	3.144(2)	116	
	C(31)-H(31B)···O(1)	2.40	3.426(3)	157	1-*x*, -½+*y*, ½-*z*
LON-IMID, 1:1:0.5 ethyl acetate solvate	N(21)_7-H(21)_7···O(2)_3	1.64	2.633(3)	167	
	N(22)_7-H(22)_7···O(1)_1	1.75	2.693(3)	153	
	N(22)_7-H(22)_7···N(2)_1	2.39	3.082(3)	125	
	N(21)_8-H(21)_8···O(1)_5	1.76	2.708(3)	155	-1+*x*, *y*, *z*
	N(21)_8-H(21)_8···N(2)_5	2.40	3.068(3)	123	-1+*x*, *y*, *z*
	N(22)_8-H(22)_8···O(2)_6	1.66	2.636(3)	162	
	N(21)_9-H(21)_9···O(2)_1	1.66	2.653(3)	166	

	N(22)_9-H(22)_9···O(1)_3	1.77	2.707(3)	153	-1+*x*, *y*, *z*
	N(22)_9-H(22)_9···N(2)_3	2.40	3.095(3)	126	-1+*x*, *y*, *z*
	N(21)_10-H(21)_10···O(2)_4	1.68	2.682(3)	171	
	N(22)_10-H(22)_10···O(1)_2	1.72	2.688(3)	159	
	N(22)_10-H(22)_10···N(2)_2	2.45	3.080(3)	120	
	N(21)_11-H(21)_11···O(1)_4	1.77	2.718(3)	155	1+*x*, *y*, *z*
	N(21)_11-H(21)_11···N(2)_4	2.38	3.055(3)	124	1+*x*, *y*, *z*
	N(22)_11-H(22)_11···O(2)_2	1.65	2.639(3)	166	
	N(21)_12-H(21)_12···O(1)_6	1.71	2.674(3)	158	
	N(21)_12-H(21)_12···N(2)_6	2.47	3.098(3)	120	
	N(22)_12-H(22)_12···O(2)_5	1.66	2.657(3)	170	
	C(6)_1-H(6)_1···O(1)_5	2.37	3.442(3)	169	*x*, ½ -*y*, -½+*z*
	C(14)_1-H(14)_1···O(31)_14	2.47	3.494(4)	157	1+*x*, ½ -*y*, -½+*z*
	C(6)_2-H(6)_2···O(1)_1	2.33	3.408(3)	174	1-*x*, 1-*y*, 1-*z*
	C(12)_2-H(12)_2···Cl(1)_4	2.69	3.597(3)	141	*x*, ½+*y*, 3/2-*z*
	C(15)_2-H(15)_2···N(2)_2	2.52	3.221(3)	121	
	C(6)_3-H(6)_3···O(1)_4	2.40	3.455(3)	165	1-*x*, 1-*y*, 1-*z*
	C(9)_4-H(9A)_4···Cl(1)_4	2.54	3.051(3)	108	
	C(15)_4-H(15)_4···N(2)_4	2.43	3.166(4)	124	
	C(9)_5-H(9B)_5···Cl(1)_5	2.53	3.069(3)	110	
	C(15)_5-H(15)_5···N(2)_5	2.50	3.223(4)	123	
	C(6)_6-H(6)_6···O(1)_3	2.32	3.392(3)	171	-1+*x*, ½-*y*, ½+*z*
	C(21)_7-H(21A)_7···O(1)_2	2.11	3.185(3)	172	
	C(21)_8-H(21A)_8···O(1)_5	2.11	3.188(3)	175	-*x*, 1-*y*, 2-*z*
	C(22)_9-H(22A)_9···O(1)_4	2.10	3.172(3)	171	
	C(22)_9-H(22A)_9···O(2)_4	2.52	3.213(3)	120	
	C(21)_10-H(21A)_10···O(1)_1	2.10	3.182(3)	176	
	C(21)_10-H(21A)···O(2)_1	2.48	3.228(3)	125	
	C(23)_10-H(23)_10···O(31A)_15	2.38	3.018(5)	116	
	C(21)_11-H(21A)_11···O(1)_3	2.11	3.190(3)	177	
	C(21)_11-H(21A)_11···O(2)_3	2.48	3.221(3)	125	
	C(21)_12-H(21A)_11···O(1)_6	2.12	3.199(3)	176	-*x*, 1-*y*, 2-*z*
LON-IMID, 2:1	O(1)-H(1)···O(1)	1.52	2.502(4)	173	1-*x*, 1-*y*, 1-*z*
	O(21)-H(21)···O(21)	1.53	2.491(4)	164	1-*x*, 1-*y*, 2-*z*
	N(41)-H(41)···(O2)	1.72	2.685(5)	159	
	N(42)-H(42)···(O22)	1.76	2.757(5)	169	
	C(9)-H(9A)···Cl(1)	2.68	3.078(4)	101	
	C(29)-H(29B)···O(1)	2.47	3.391(5)	142	*x*, *y*, 1+*z*
	C(41)-H(41A)···N(21)	2.42	3.289(7)	136	1-*x*, 1-*y*, 2-*z*
LON-IMID, 1:1	O(1)-H(1)···O(1)	1.56	2.540(3)	177	2-*x*, -*y*, 2-*z*
	N(41)-H(41)···O(21)	1.80	2.764(3)	160	1-*x*, 1-*y*, 1-*z*
	N(41)-H(41)···N(22)	2.46	3.119(3)	122	1-*x*, 1-*y*, 1-*z*
	N(42)-H(42)···N(42)	1.62	2.627(3)	178	1-*x*, -*y*, -*z*
	N(45)-H(45)···O(21)	1.57	2.563(17)	166	1-*x*, 1-*y*, 1-*z*
	N(46)-H(46)···O(1)	1.67	2.673(6)	170	1-*x*, 1-*y*, 1-*z*

	C(9)-H(9A)···Cl(1)	2.66	3.067(2)	101	
	C(9)-H(9A)···O(22)	2.46	3.499(3)	160	
	C(41)-H(41A)···O(22)	2.28	3.158(3)	137	*x*, *y*, -1+*z*
	C(45)-H(45A)···O(22)	2.36	2.992(7)	116	1-*x*, 1-*y*, 1-*z*
	C(45)-H(45A)···N(2)	2.42	3.084(6)	118	1-*x*, 1-*y*, 1-*z*
	C(46)-H(46A)···O(2)	2.28	3.015(9)	124	-1+*x*, 1+*y*, -1+*z*
LON-ISO	O(2)-H(2)···N(22)	1.66	2.6366(19)	176	3/2-*x*, ½+y, ½-*z*
	N(21)-H(21A)···O(21)	2.30	3.241(2)	156	3/2-*x*, ½+*y*, 3/2-*z*
	N(21)-H(21B)···O(1)	1.96	2.971(2)	175	½+*x*, 3/2-*y*, ½+*z*
	C(9)-H(9A)···Cl(1)	2.66	3.1010(17)	104	
	C(9)-H(9B)···O(21)	2.22	3.287(2)	169	1-*x*, 1-*y*, 1-*z*
	C(23)-H(23)···O(1)	2.22	3.196(2)	149	½+*x*, 3/2-y, ½+*z*
	C(25)-H(25)···Cl(2)	2.73	3.5535(17)	132	*x*, -1+*y*, *z*
	C(26)-H(26)···O(21)	2.34	3.350(2)	155	3/2-*x*, -½+*y*, 3/2-*z*
LON-MEL	N(21)-H(21)···O(1)	1.70	2.6538(18)	157	
	N(24)-H(24A)···N(2)	2.01	3.0093(19)	171	
	N(24)-H(24B)···O(1)	2.44	3.3959(19)	157	-1+*x*, *y*, *z*
	N(25)-H(25A)···N(23)	1.91	2.9177(19)	175	2-*x*, 2-*y*, 1-*z*
	N(25)-H(25B)···O(2)	2.06	2.7888(18)	127	-1+*x*, 1+*y*, *z*
	N(26)-H(26A)···O(1)	2.18	3.0084(19)	138	
	N(26)-H(26B)···O(2)	1.99	2.9891(18)	173	3-*x*, 1-*y*, 1-*z*
	C(9)-H(9A)···Cl(1)	2.64	3.0610(16)	103	
LON-NICO	O(2)-H(2)···O(21)	1.56	2.531(3)	169	
	N(21)-H(21A)···O(1)	2.23	2.852(3)	119	1-*x*, 1-*y*, 1-*z*
	N(21)-H(21B)···O(1)	1.97	2.960(4)	168	
	C(4)-H(4)···O(2)	2.48	3.000(4)	108	
	C(7)-H(7)···Cl(1)	2.67	3.679(3)	155	
	C(9)-H(9A)···Cl(1)	2.50	3.091(3)	113	
	C(9)-H(9B)···N(22)	2.43	3.463(4)	158	1-*x*, 1-*y*, 1-*z*
	C(15)-H(15)···N(22)	2.46	3.445(4)	151	1-*x*, 2-*y*, 1-*z*
	C(26)-H(26)···O(21)	2.47	3.239(4)	127	1-*x*, ½+*y*, ½-*z*
LON-PIPE	N(51)-H(51A)···O(22)	1.71	2.691(3)	164	
	N(51)-H(51B)···O(1)	1.68	2.644(3)	159	
	N(51)-H(51B)···N(2)	2.52	3.112(3)	117	
	N(61)-H(61A)···O(21)	1.69	2.688(3)	172	
	N(61)-H(61B)···O(1)	2.34	3.000(3)	122	-1+*x*, *y*, *z*
	N(61)-H(61B)···O(2)	1.77	2.754(3)	163	-1+*x*, *y*, *z*
	C(9)-H(9A)···Cl(1)	2.59	3.063(3)	106	

	C(14)-H(14)···Cl(21)	2.65	3.655(4)	154	1+*x*, *y*, *z*
	C(27)-H(27)···Cl(21)	2.65	3.665(2)	155	
	C(29)-H(29B)···Cl(21)	2.54	3.132(3)	113	
	C(52)-H(52A)···O(21)	2.32	3.360(3)	160	1-*x*, 2-*y*, 2-*z*
	C(62)-H(62B)···O(1)	2.38	3.033(3)	117	1+*x*, *y*, *z*

* D = Donor, A = Acceptor

Table 7.2.2. Interactions for crystal structures containing non-pharmaceutically acceptable co-formers

Sample	D–H···A*	H···A /Å	D···A /Å	D–H···A /°	Symmetry code
LON-2APD, acetonitrile solvate	N(21)-H(21A)···O(1)	1.84	2.838(2)	171	
	N(21)-H(21B)···O(1)	1.80	2.795(3)	168	*x*, ½-*y*, ½+*z*
	N(22)-H(22)···O(2)	1.65	2.648(2)	168	x, ½-y, ½+z
	C(9)-H(9A)···O(1)	2.37	3.329(3)	146	x, ½-y, ½+z
	C(9)-H(9A)···N(2)	2.54	3.492(3)	146	x, ½-y, ½+z
LON-2APD, 1:1:1 ethyl acetate solvate	N(21)-H(21A)···O(1)	1.85	2.856(3)	177	*x*, 2-*y*, ½+*z*
	N(21)-H(21B)···O(1)	1.78	2.779(3)	168	*x*, *y*, 1+*z*
	N(22)-H(22)···O(2)	1.66	2.665(3)	170	*x*, *y*, 1+*z*
	C(9)-H(9B)···O(1)	2.49	3.451(4)	147	*x*, 2-*y*, ½+*z*
	C(23)-H(23)···Cl(2)	2.71	3.643(3)	144	-1+*x*, 2-*y*, -½+*z*
	C(25)-H(25)···O(31)	2.40	3.171(4)	127	-1+*x*, *y*, *z*
LON-2APM	O(2)-H(2)···N(22)	1.66	2.634(3)	169	
	N(23)-H(23A)···N(2)	2.06	3.059(3)	169	1-*x*, 1-*y*, 1-*z*
	N(23)-H(23B)···O(1)	1.89	2.889(3)	169	
	N(33)-H(33A)···N(32)	1.97	2.977(3)	178	*x*, ½-*y*, ½+*z*
	N(33)-H(33B)···N(31)	2.12	3.123(3)	172	*x*, ½-*y*, -½+*z*
LON-246TAPM	N(22)-H(22)···O(2)	1.69	2.663(2)	159	1+*x*, *y*, *z*
	N(23)-H(23A)··· N(21)	1.94	2.943(2)	174	1-*x*, 1-*y*, 1-*z*
	N(23)-H(23B)··· O(2)	2.35	2.997(2)	121	*x*, *y*, 1+*z*
	N(24)-H(24A)···O(1)	2.18	2.987(2)	136	1+*x, y, z*
	N(24)-H(24B)···O(2)	1.94	2.932(2)	166	-1+*x*, *y*, -1+*z*
	N(25)-H(25A)···N(2)	2.00	2.986(2)	166	1-*x*, 1-*y*, -*z*
	N(25)-H(25B)···O(2)	2.00	2.927(2)	152	1+*x*, *y*, 1+*z*
	C(9)-H(9B)···Cl(1)	2.57	3.1450(19)	112	
LON-4DMAP, 2:1	O(1)-H(1)···O(21)	1.50	2.477(2)	173	
	O(1)-H(1)···O(22)	2.60	3.145(2)	115	
	N(41)-H(41)···O(22)	1.72	2.675(4)	157	
	N(41A)-H(41B)···O(2)	2.00	2.830(4)	138	2-*x*, -*y*, 2-*z*
	N(41A)-H(41B)···O(21)	2.43	3.135(4)	126	2-x, -y, 2-z

	C(24)-H(24)···O(22)	2.54	3.076(3)	110	
	C(30)-H(30B)···O(22)	2.44	3.459(2)	157	-1+*x*, *y*, *z*
	C(41)-(H41A)···N(2)	2.23	3.283(15)	163	
	C(41A)-H(41C)···N(22)	2.35	3.430(16)	173	2-x, -y, 2-z
	C(45A)-H(45A)···O(2)	2.55	3.058(17)	108	2-x, -y, 2-z
	C(46)-H(46A)···O(22)	2.15	3.166(11)	155	4-x, 1-y, 1-z
	C(46A)-H(46F)···O(2)	2.17	3.196(16)	157	
	C(47)-H(47C)···O(1)	2.34	3.145(14)	130	4-x, 1-y, 1-z
	C(47A)-H(47F)···O(21)	2.30	3.294(17)	152	
LON – 4DMAP, 1:1 salt dihydrate	N(21)-H(21)···O(1)	1.67	2.6279(16)	156	
	O(21)-H(21B)···O(1)	1.76	2.7383(14)	173	
	O(21)-H(21C)···O(22)	1.76	2.7406(18)	176	½-*x*, ½+*y*, ½-*z*
	O(22)-H(22A)···O(2)	1.76	2.7210(16)	164	
	O(22)-H(22B)···O(21)	1.89	2.8102(18)	155	
	C(4)-H(4)···O(2)	2.53	3.0646(17)	109	
	C(9)-H(9A)-O(21)	2.44	3.4738(17)	160	1-*x*, 1-*y*, 1-*z*
	C(11)-H(11)···O(21)	2.41	3.3927(14)	150	1-*x*, 1-*y*, 1-*z*
LON-4,4BIPY	O(1)-H(1)···N(81)	1.61	2.565(4)	164	
	O(21)-H(21)···N(82)	1.61	2.575(4)	167	
	O(41)-H(41)···N(91)	1.56	2.543(4)	176	
	O(61)-H(61)···N(92)	1.62	2.593(4)	169	
	C(9)-H(9B)···O(1)	2.35	3.398(8)	162	*x*, ½-*y*, -½+*z*
	C(27)-H(27)···Cl(21)	2.58	3.569(4)	151	*x*, ½-*y*, ½+*z*
	C(29)-H(29B)···Cl(21)	2.62	3.076(5)	105	
	C(29)-H(29B)···O(21)	2.39	3.436(5)	163	*x*, ½-*y*, ½+*z*
	C(49)-H(49A)···Cl(41)	2.66	3.071(4)	102	
	C(49)-H(49A)···O(61)	2.34	3.405(5)	167	2-*x*, 1-*y*, -*z*
	C(69)-H(69A)···O(41)	2.43	3.475(8)	161	2-*x*, 1-*y*, -1-*z*
	C(69)-H(69A)···N(42)	2.56	3.396(8)	133	2-*x*, 1-*y*, -1-*z*
	C(91)-H(91)···O(61)	2.53	3.220(4)	121	2-*x*, 1-*y*, -1-*z*

* D = Donor, A = Acceptor

7.3. Crystal structure solution, refinement details, and discussion

7.3.1 LON-HALO 1:1 salt trihydrate

The LON-HALO.3H_2O salt has a 1:1 stoichiometry and crystallises in space group *I*2/*a* containing three water molecules. Two of these water molecules sites display disorder in approximate ratios In addition to the primary interactions, each HALO forms a further two interactions. One interaction (O-H···O) occurs from a water molecule of a self-assembling water molecule tetramer (arranged almost perpendicular to the original tetramer and

parallel to the dichlorine-substituted ring of LON). The second interaction occurs from the haloperidol hydroxyl group to a water molecule (O-H···O) located in a second tetramer of LON and water molecules (Figure 28).

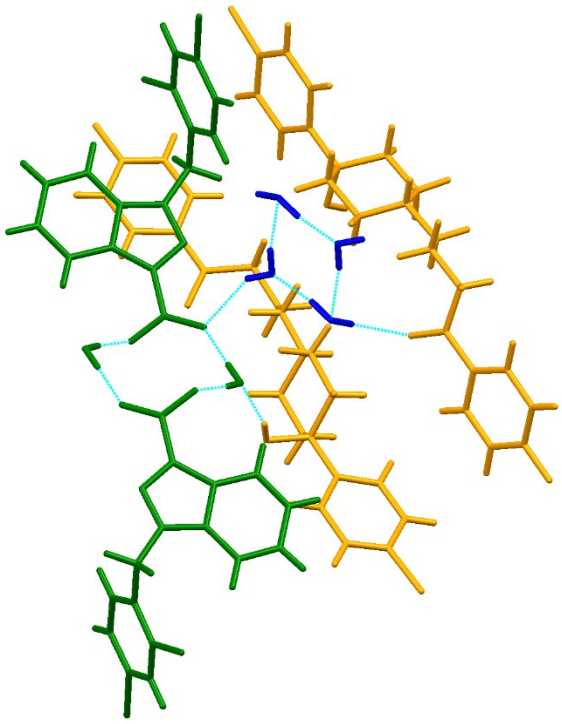

Figure 28. One unit of LON-HALO.3H_2O showing the tetrameric motifs (water: blue, LON-water: green) and interactions between them and the HALO molecules (orange).

7.3.2 LON-IMID salts

IMID forms a salt with LON in three forms; a 1:1:0.5 ethyl acetate (LON-IMID.0.5EtOAc) salt solvate, a 1:1 salt and a 2:1 hybrid structure. LON-IMID.0.5EtOAc crystallises in monoclinic $P2_1/c$ space group; 15.1 Å, 29.9 Å, 26.9 Å, β = 97.6°. The asymmetric unit contains 6 molecules of both deprotonated LON and protonated IMID and 3 ethyl acetate solvent molecules. Disorder is present in the central solvent molecule in an approximate ratio 55:45 and in two of the six dichlorine-substituted aromatic rings of LON (residues 4 and 5) in

approximate ratios 75:25 and 80:20 respectively. Further disorder also occurs in other dichlorine-substituted rings of LON, arising from varying angles of rotation around the C9-C10 bond. This disorder was seen to be at a very low level when modelling was attempted (~94:6 ratio) and did not add significantly to the model therefore is not included in the final structure. The disordered ethyl acetate molecule contains few interactions to maintain a single position and orientation of the solvent molecule and due to the symmetrical shape it can fit in the space with no preference for either orientation.

The structures of 2:1 and 1:1 ratios were obtained from the same crystallisation set up. The 2:1 structure crystallises in the triclinic space group $P\bar{1}$ containing two molecules of LON and one of IMID hence, it forms a hybrid co-crystal-salt structure. It displays a non-merohedral twin at 36% and contains solvent accessible voids of 110 $Å^3$ (Figure 29). Solvent molecules may be located within these however; residual electron density indicates no solvent molecules. Possible solvents are methanol, acetonitrile or water molecules.

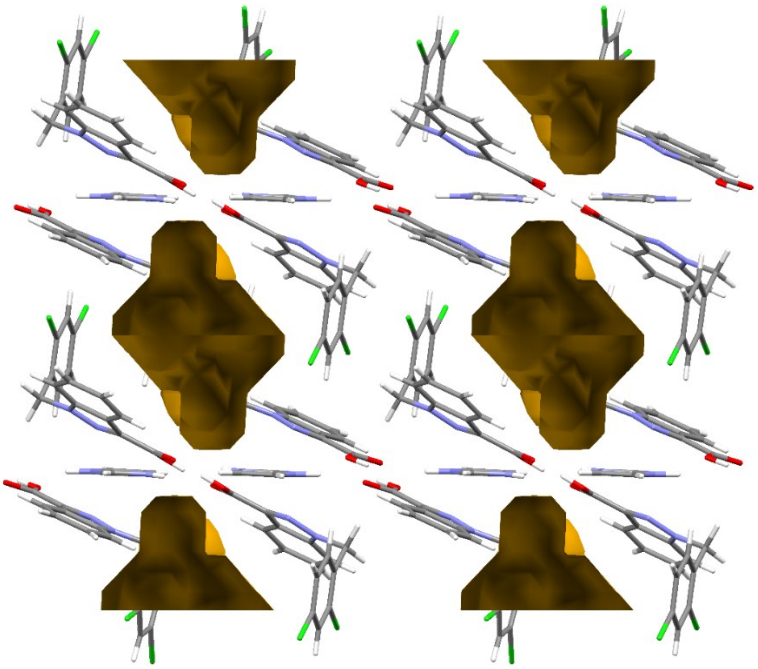

Figure 29. LON-IMID 2:1 structure viewed down *b* displaying voids in which solvent molecules may be contained.

The 1:1 LON-IMID salt contains two independent units of each species in the asymmetric unit. One IMID is protonated, occupancy 0.5 average charge +0.5, which charge balances with one partially deprotonated LON. The second LON contains a fully deprotonated carboxylate which is charge balanced by the second (protonated) IMID. This IMID contains full molecule disorder over two positions, in an approximate 50:50 ratio.

No void space is present in this structure, which was obtained from the same crystallisation set up as the 2:1 ratio structure but at a later date. It is therefore hypothesised that this 1:1 structure may be related to the 2:1 structure with void space collapse. The two structures are overlaid in Figure 30.

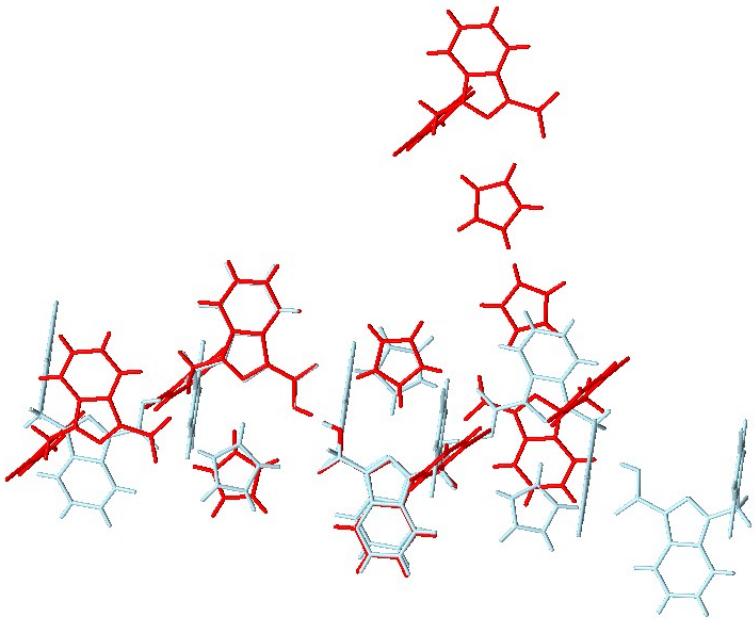

Figure 30. Overlay of section of LON IMID 1:1 (red) and 2:1 (light blue) structures.

7.3.3 LON-NICO 1:1 co-crystal

The LON-NICO co-crystal crystallises in a monoclinic space group, $P2_1/c$ and was seen to be pseudo-merohedrally twinned at 3.5% with twin law 0 1 0 0 0 -1 0 0 0 1.

7.3.4 LON-PIPE salt

PIPE forms a 2:1 salt with LON which crystallises in the triclinic space group $P\bar{1}$ and displays non-merohedral twinning in an approximate ratio 54:46. The asymmetric unit contains two moieties of LON and two half moieties of PIPE which each have an occupancy of 0.5 and are located on inversion centres. A ladder motif is seen, which stack in a regular array. Parallel ladders occur on the vertices of the unit cell to give a grid-type packing.

7.3.5 Remaining structures

All remaining structures containing pharmaceutical co-formers formed 1:1 constructs and are free from disorder.

8. ΔpK_a Predictions of Co-Crystal/Salt Formation

The pK_a values for the co-former molecules are depicted in Table 7.1, determined by the physiochemical properties calculator plugin[7] in ChemAxon's MarvinSke[8] software along with the ΔpK_a (pK_a (conjugate acid of base) – pK_a (carboxylic acid) when analysed with respect to LON. Two values for LON are used, one calculated using the same method as applied to the co-formers and a second taken from literature (not all values for co-formers were found in the literature therefore calculated values were used for all for consistency). Associated predictions based on the rule of three (>3 = salt, 0-3 hard to predict, <0 co-crystal) and experimental observations are also shown and are indicated by C, co-crystal; S, salt, SC, salt-co-crystal hybrid, and I, intermediate range where predictions are difficult.

Table 8.1 pK_a values for all successful co-formers with ΔpK_a when analysed with respect to LON, predicted experimental outcome and experimental results obtained.

Co-former	pK_a (Marvinsketch predicted)	ΔpK_a (LON value 3.02[a])	Prediction	ΔpK_a (LON value 4.35[b])	Prediction	Experimental results
246TAPYM	7.28	4.26	S	2.93	I	Salt
2APYD	6.84	3.82	S	2.49	I	Salt
2APYM	3.62	0.6	I	-0.73	C	Co-Crystal
4,4BIPY	4.44	1.42	I	0.09	I	Co-Crystal
4DMAP	8.78	5.76	S	4.43	S	Salt/Co-Crystal Salt
BENZ	-0.36	-3.38	C	-4.71	C	Co-Crystal
HALO	8.05	5.03	S	3.7	S	Salt
IMID	6.97	3.95	S	2.62	I	Salt/Partial/Co-Crystal Salt
ISO	3.45	0.43	I	-0.9	C	Co-Crystal
MEL	8.56	5.54	S	4.21	S	Salt
NICO	3.63	0.61	I	-0.72	C	Co-Crystal
PIPE	5.18	2.16	I	0.83	I	Salt

[a] from physiochemical properties calculator plugin in MarvinSketch

[b] reported literature value[9]

9. Stability

9.1 Accelerated stability (13 weeks, 40 °C / 75 % RH) testing for materials containing pharmaceutically acceptable co-formers.

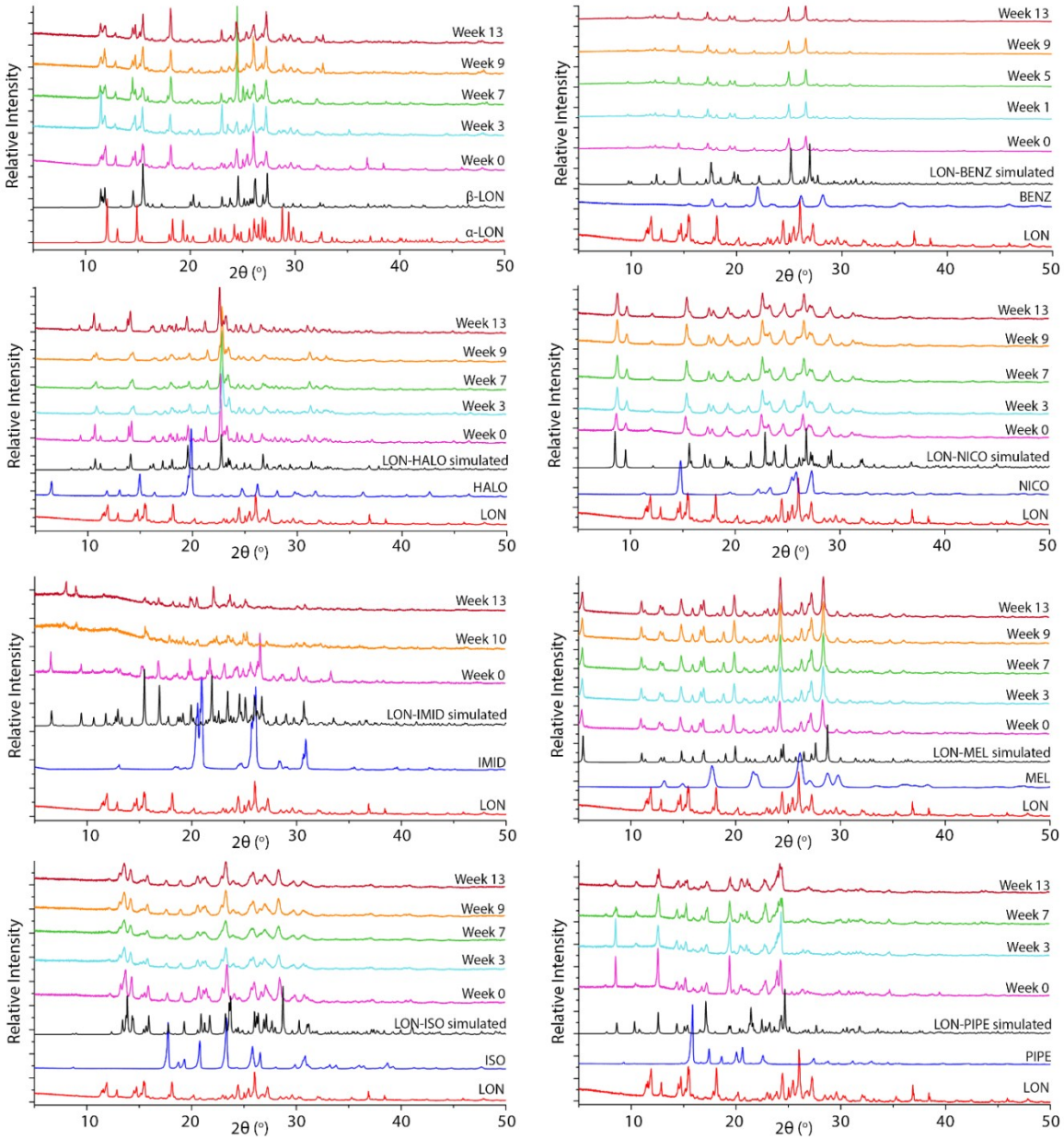

Figure 31. Stacked PXRD patterns for storage under accelerated conditions (45 °C / 75 % RH) for lonidamine parent material and six new materials. Data indicates that all samples are stable when subjected to such conditions except for the imidazole salt solvate.

9.2 Slurry (24 hours, RT, 1% Tween 80 ® in aqueous solution)

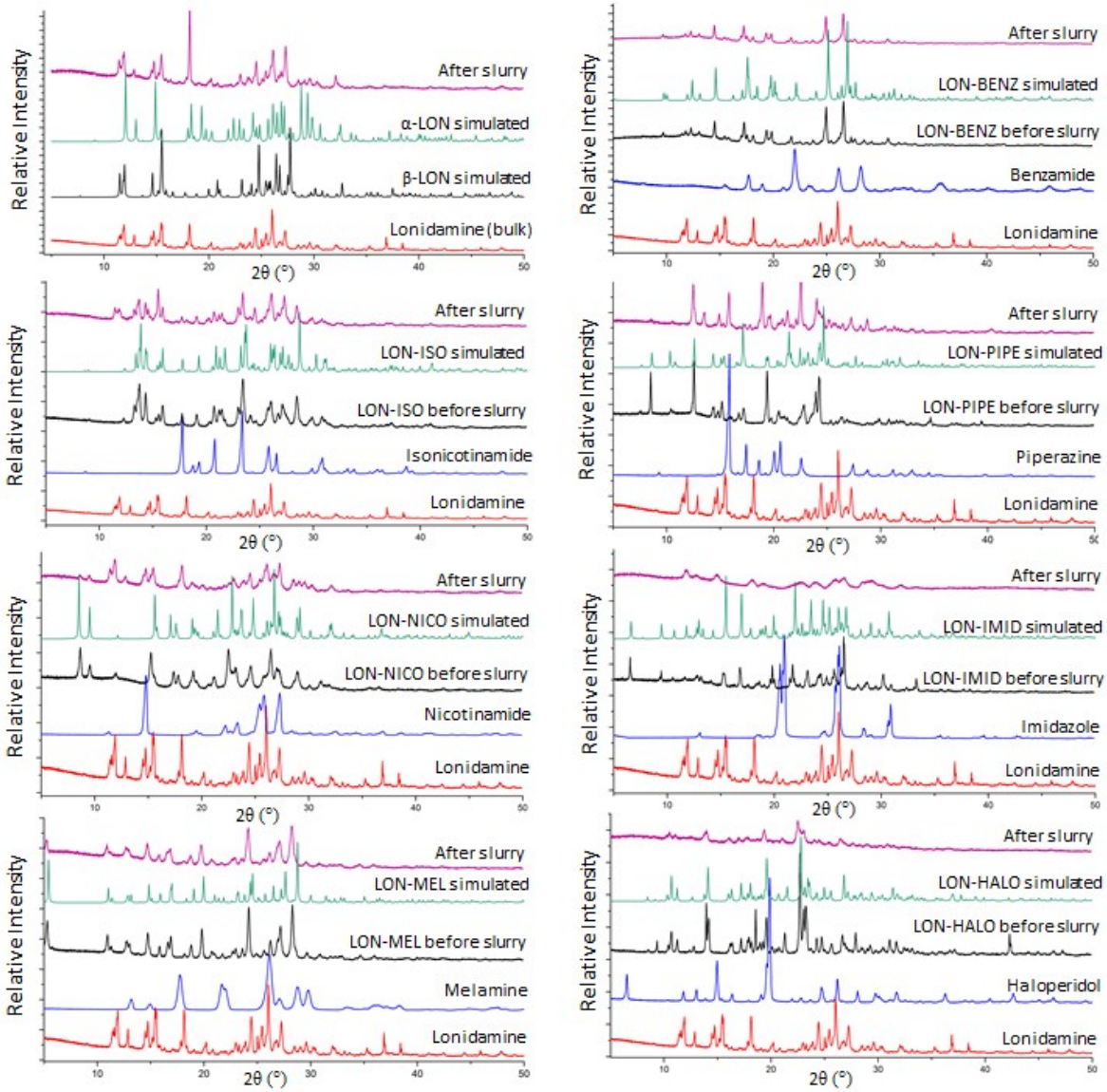

Figure 32. Overlays of PXRD patterns resulting from slurry experiments at room temperature in 1% Tween 80 ® aqueous solution. Data indicates that LON, the co-crystal with BENZ and the salts with HALO, MEL, PIPE are stable under these conditions. The co-crystals with NICO and ISO however undergo partial disociation and LON-IMID.0.5EtOAc salt solvate does not withstand the conditions resulting in a poorly crystalline material which resembles parent API.

10.Thermal Properties

10.1 Hot Stage Microscopy (HSM)

A number of samples displayed some interesting behaviour in DSC, in addition to the melting endotherm of the co-crystal/salt. These were investigated using hot stage microscopy (HSM)

10.1.1 LON-HALO.3H_2O salt

LON-HALO.3H_2O DSC shows a jagged endotherm (100-125 °C) preceded by a small broad endotherm (50-80 °C). These are attributed to water loss (broad endotherm) and melting due to lattice breakdown upon further water removal (100-125 °C). Water loss from hydrated crystal structures can be complex: different sites, location within crystal and interactions can all play a part. It is hypothesised that water loss is a staggered event, combined with a staged melting and gives the endotherm observed in the DSC. HSM investigation (Figure 33) indicated water loss and melting occurring simultaneously over a broad temperature range, with degradation at 275 °C (also evident in the DSC).

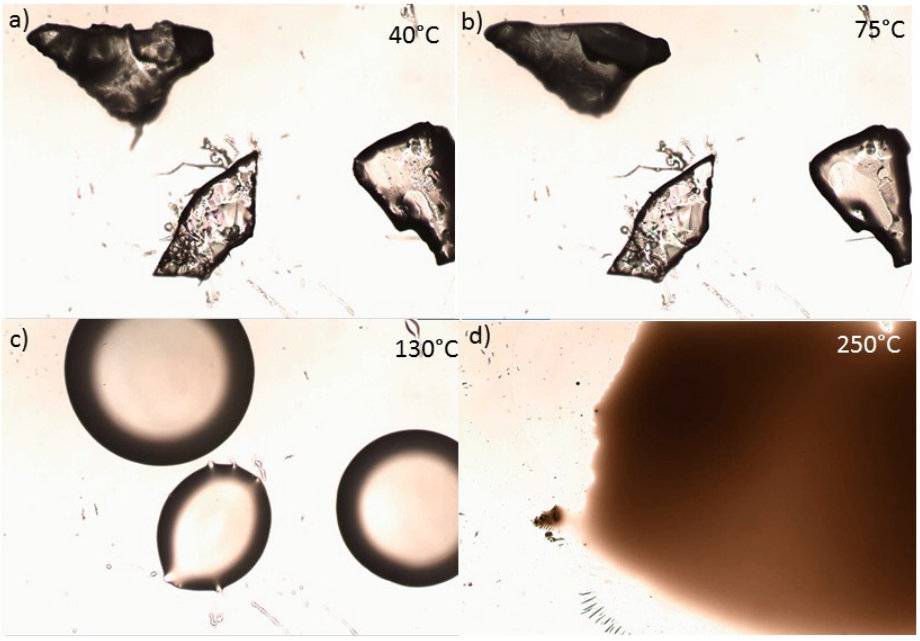

Figure 33. Images from HSM investigation into LON-HALO.3H_2O salt showing a) sample initially, b) water loss onset, c) melt and d) decomposition.

10.1.2 LON-IMID.0.5EtOAc salt

LON-IMID.0.5EtOAc DSC shows an endotherm at 81 °C with a second event occurring at much higher temperature (over 275 °C). The first event is attributed to solvent loss with concomitant melting due to lattice breakdown from solvent removal, as evidenced in HSM (Figure 34). The second event was observed in HSM as some degradation of the melt (darkening of the sample, likely to be IMID degradation).

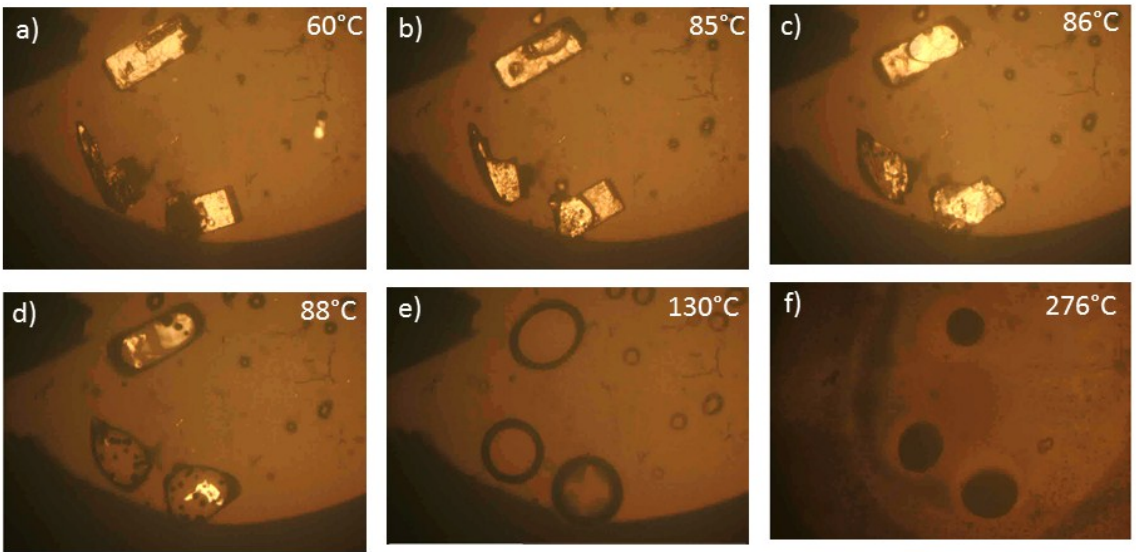

Figure 34. Images from HSM investigation into LON-IMID.0.5EtOAc salt showing a) sample initially, b) solvent loss and melting onset, c-e) melt f) decomposition.

10.2 Thermal Gravimetric Analysis (TGA)

TGA was used to further investigate LON-HALO.3H_2O, LON-IMID.0.5EtOAc and the two non-pharmaceutically acceptable LON-2APYD salts as all samples contained solvent / water molecules. The DSC for LON-HALO.3H_2O exhibited complex thermal behaviour, and whilst HSM gave a visual insight into this TGA can provide an additional, quantitative, analysis.

10.2.1 LON-HALO.3H_2O

The TGA (Figure 35) indicates an initial weight loss of 6.42 % up to 120 °C which corresponds to the loss of the three water molecules (7.19 % by weight of the compound) and evidenced in the HSM and DSC experiments (Figures 33 and 36). A further 12.74 % decrease in mass occurs between 120 °C and 250 °C followed by significant mass change which corresponds to sample degradation.

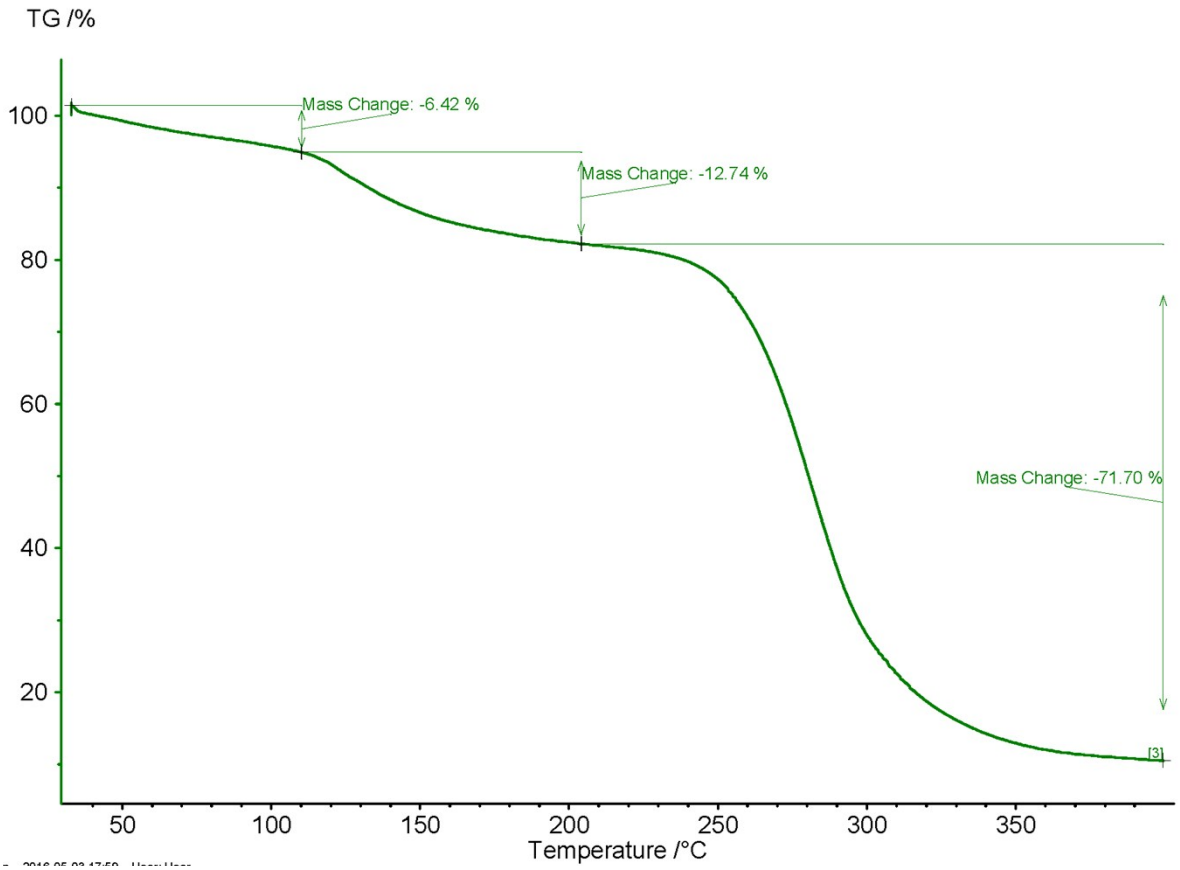

Figure 35. TGA for LON-HALO.3H_2O 25-400°C at 10 °C min^{-1} showing water loss followed by sample degradation.

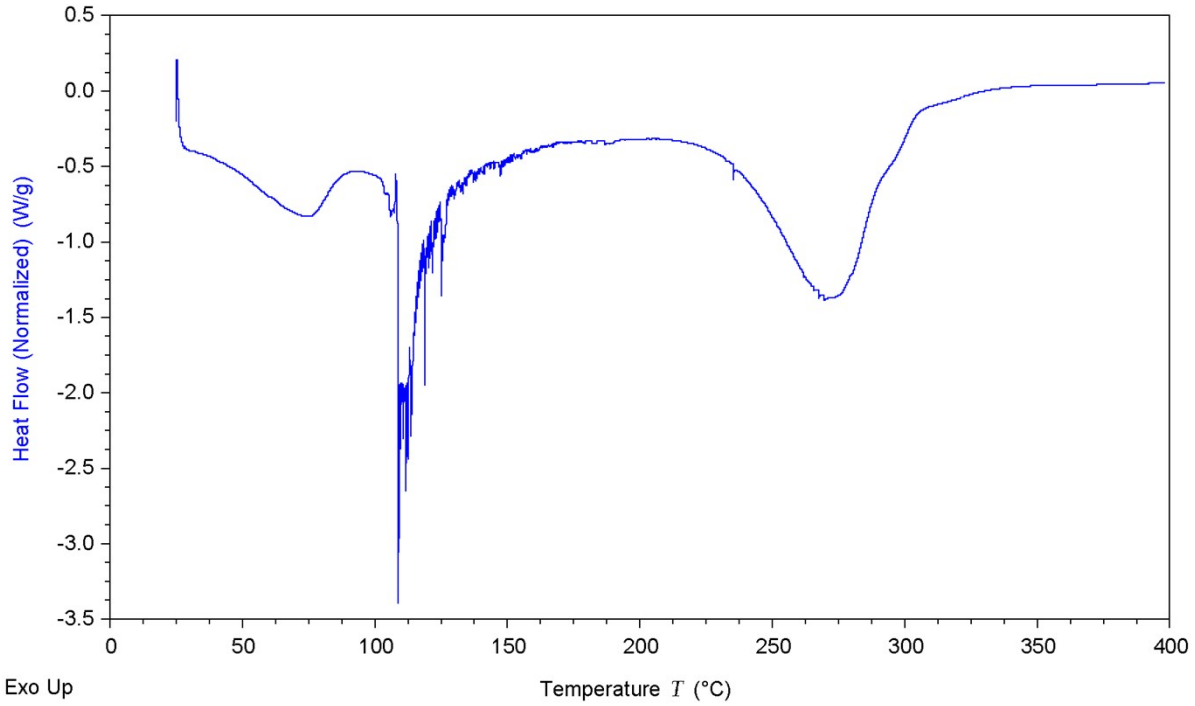

Figure 36. DSC of LON-HALO.3H_2O salt, 25-400 °C at 10 °C min^{-1}. The baseline is not as expected for a usual DSC trace however this is reproducible and ascribed to hydrate behaviour when heated (which is known to be complex and often non-conforming to standard, expected behaviours).

10.2.2 LON-IMID.0.5EtOAc

LON-IMID ethyl acetate solvate (1:1:0.5) contains 10.7 % solvent by mass. The TGA (Figure 37) indicates an initial weight loss of 1.39 % up to 100 °C followed by a gradual and steady mass loss until 250 °C. This corresponds to some initial solvent loss (before 100 °C) which disrupts the hydrogen bonding network and causes simultaneous melting with further solvent loss. After 250 °C a significant and sharp mass change is observed which corresponds to sample degradation.

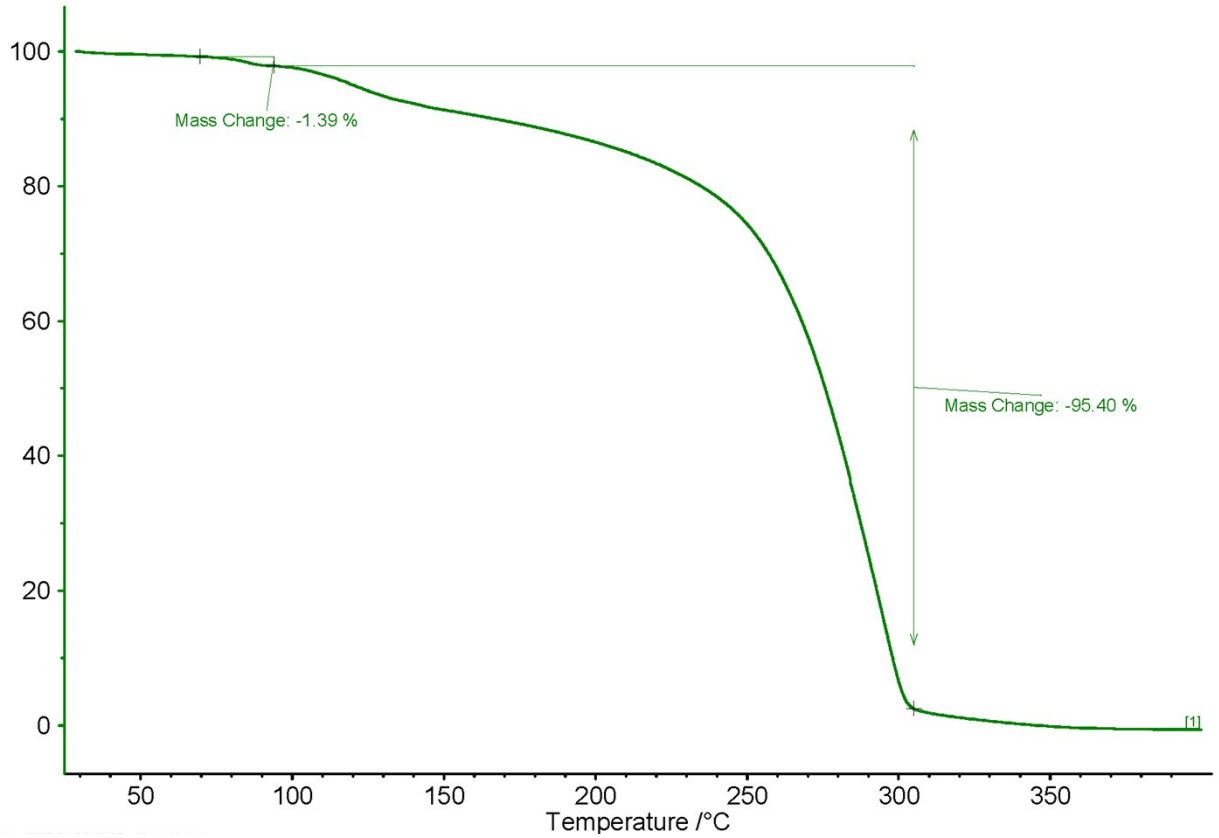

Figure 37. TGA for LON-IMID.0.5EtOAc salt 25-400°C at 10 °C min^{-1} showing solvent loss occurs concomitantly with melting and sample degradation.

10.2.3 LON-2APYD

The TGA for the two LON-2APYD salts are depicted in figures 38 and 39. Figure 38 shows the TGA for the ethyl acetate salt (1:1:1 ratio) with solvent loss in the expected temperature range for ethyl acetate (bp 77 °C). This % mass loss is in agreement with the stoichiometry determined by SCXRD as a 1:1:1 ratio would contain ethyl acetate at 17.5 % by mass. Following solvent loss a small gradual mass loss is seen followed by degradation (onset 250 °C). The TGA for the second salt (Figure 39) indicates a mass loss between 80-90 °C, representative of solvent loss and corresponding to the supposed acetonitrile (bp 82 °C) from void space analysis and electron count.

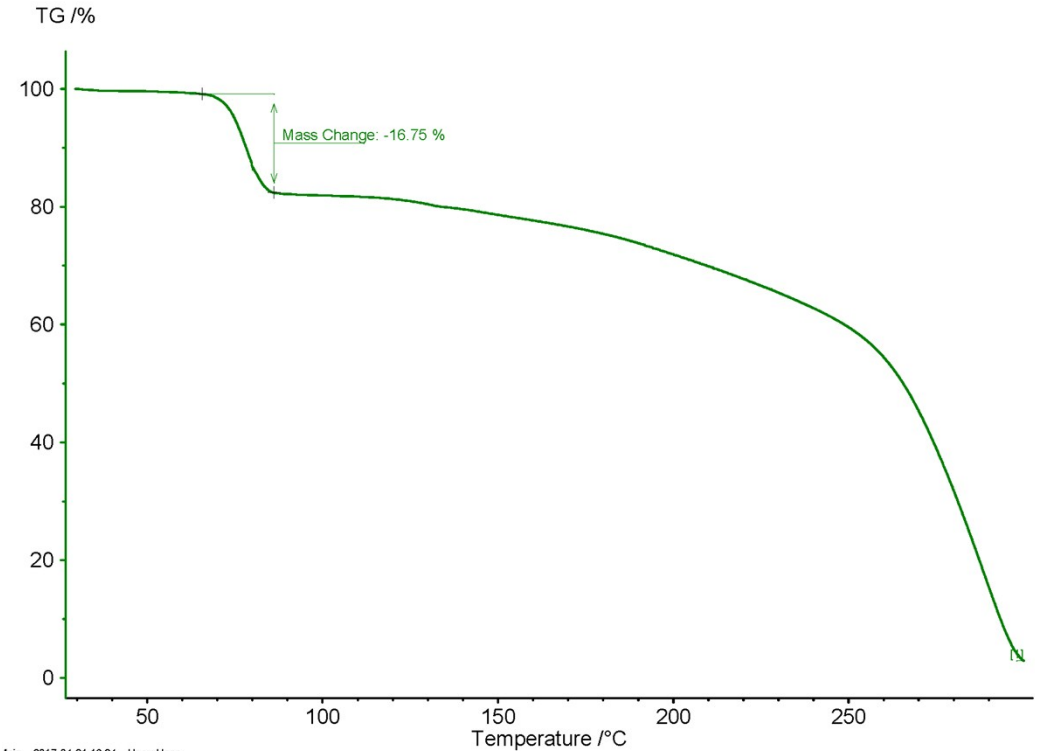

Figure 38. TGA for LON-2APYD.EtOAc solvate 30-300°C at 10 °C min^{-1} showing solvent loss at the expected temperature for ethyl acetate followed sample degradation from 250°C.

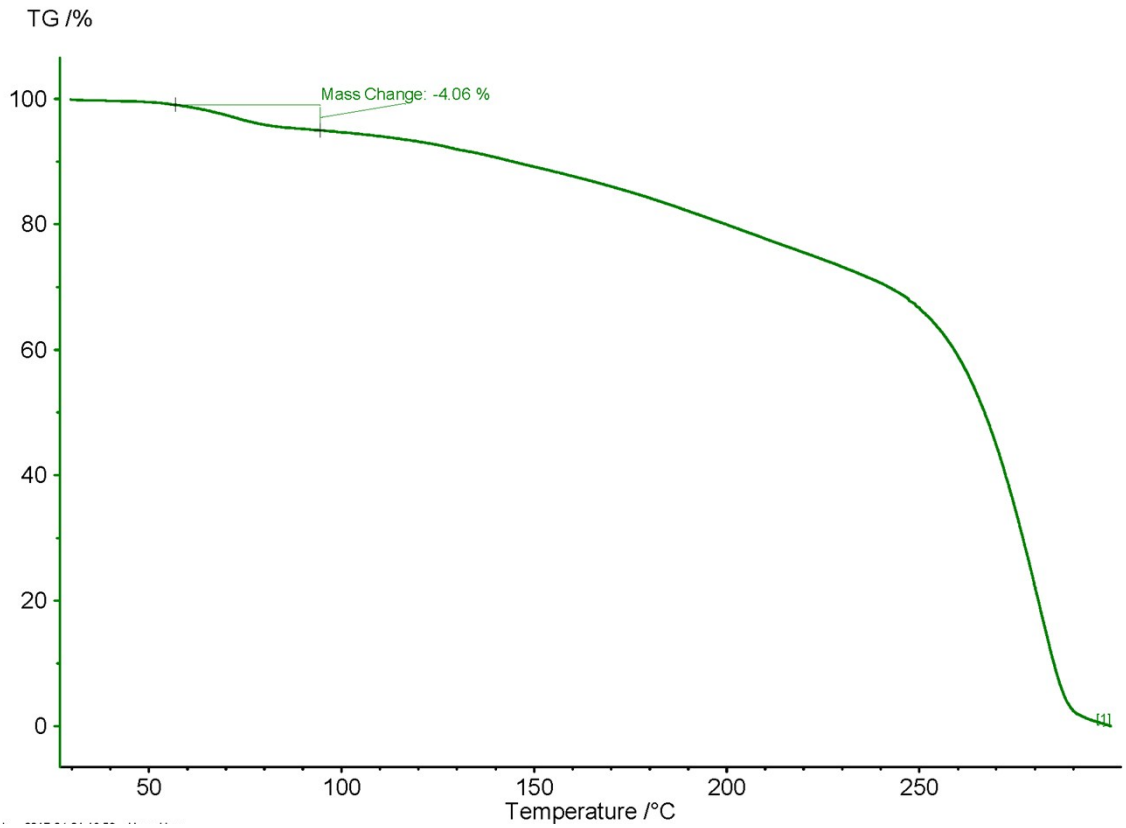

Figure 39. TGA for LON-2APYD acetonitrile solvate 30-300°C at 10 °C min^{-1} showing solvent loss at the expected temperature for acetonitrile, followed sample degradation from 250°C.

10.2.4 LON-4DMAP.2H_2O

The TGA for the LON-4DMAP dihydrate is depicted in figure 40. The mass loss is in agreement with the dihydrate determined by SCXRD, with two water molecules equating to a mass of 7.5 % by weight. Following dehydration, completed by 100 °C, the sample appears to degrade after melting (degradation onset 250 °C).

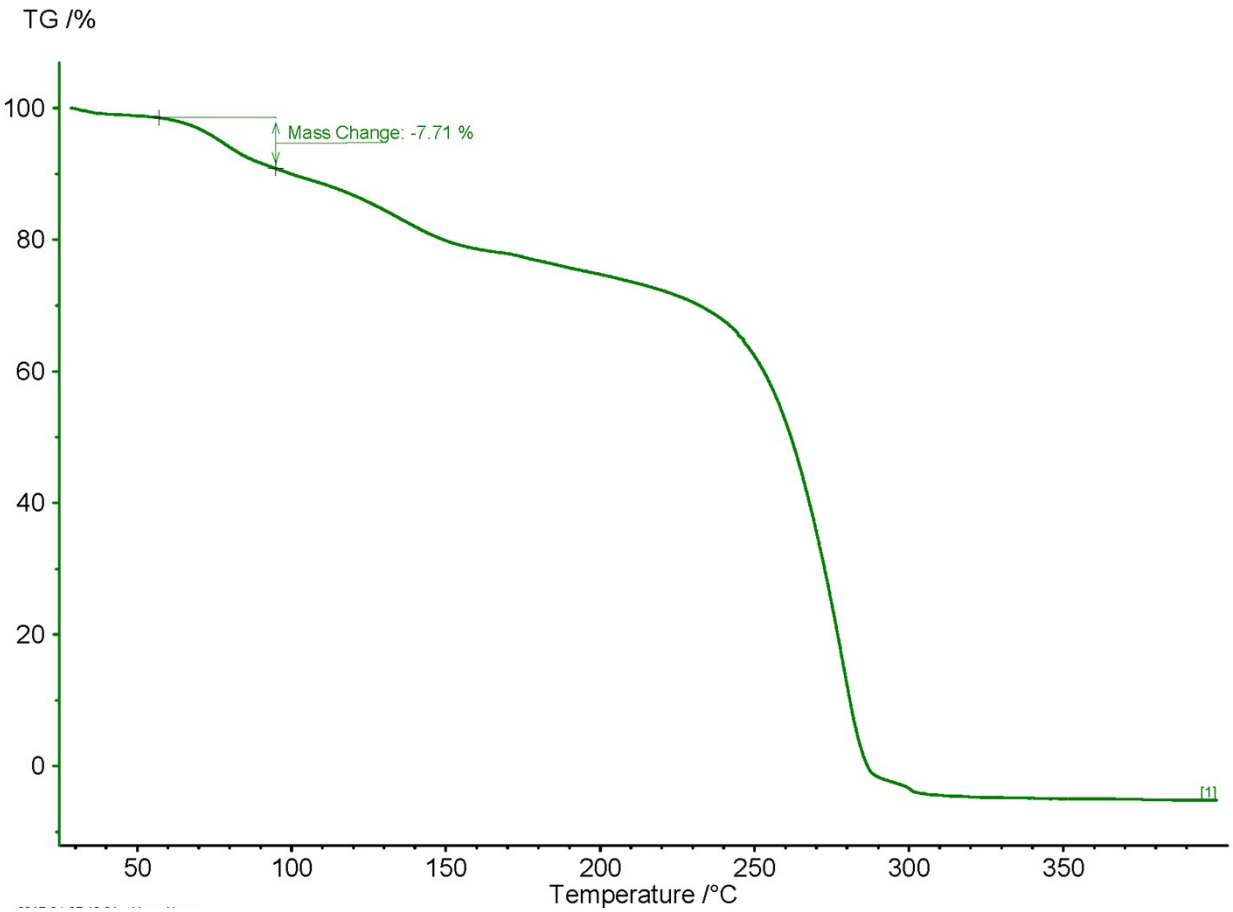

Figure 40. TGA for LON-4DMAP.2H_2O 30-400°C at 10 °C min^{-1} showing water loss equating to two molecules by 100 °C, followed sample degradation from 250°C.

11. Experimental

Hot Stage Microscopy (HSM). Hot stage microscopy was used to visually observe some of the events seen through DSC analysis. This was carried out using a Leica DM2500 microscope fitted with Lumenera Infinity 1 CMOS digital microscope camera and Mettler

Toledo FP82HT Hot Stage with FP90 Central Processor. Data capture was completed using Studio Capture software v3.1. Experimental parameters, such as temperature range and heating rate, were tailored to each experiment to focus on particular events but typically mimicked the DSC set up to allow comparisons to be made.

Thermal Gravimetric Analysis (TGA). Thermal gravimetric analysis was used to investigate some observations in DSC and HSM. A Netzsch TGA 209 F1 Libra was used with a ramp rate of 10 °C min^{-1} from 25 °C up to a maximum of 400 °C (depending on the nature of the sample and observations from DSC).

Single crystal X-ray diffraction SCXRD.

Data for the LON-4,4BIPY co-crystal were collected on a Rigaku FRE+ equipped with VHF Varimax confocal mirrors, an AFC10 goniometer and an HG Saturn724+ detector using Mo-Kα radiation (λ = 0.71075 Å). Crystal Clear 3.1[10] software was used for data collection and CrysAlisPro[11] for data reduction and Gaussian absorption correction. Data for the remaining samples were collected on an Agilent Technologies Dual Source Supernova, four-circle diffractometer fitted with CCD detector and graphite monochromator using Mo-Kα radiation (λ = 0.71073 Å). CrysAlisPro software was used for data collection, reduction and absorption correction using face indexing and Gaussian corrections. All data was collected at 100K and suitable crystals selected and mounted using paratone or fomblin oil on a MiTeGen Micromesh holder. Structure solution for all was carried out using Direct Methods in SHELXT[12] and refined using full-matrix least squares on F2 using SHELXL 2014[13] both implemented in the Olex2[14] software. Non-hydrogen atoms were refined with anisotropic displacement parameters. Hydrogen atoms for heteroatoms (N and O) were located from the difference Fourier map and freely refined. The remaining protons, including those of

water molecules in hydrate structures were fixed in idealised positions with their displacement parameters riding on the values of their parent atoms.

Various restraints and constraints were used in the structure refinement for LON-4,4BIPY 2:1 co-crystal to give the optimum structure. The SMTBX solvent masking routine as implemented in Olex2 was used for the 1:1 LON-2APYD acetonitrile solvate as this was seen to be located in voids with no apparent hydrogen bonding to maintain a fixed position of the solvent molecules.

12. References

1. F. Benetollo, A. Pra, F. Orsini and L. Baiocchi, *J. Crystallogr. Spectrosc. Res.,* **1993,** *23*, 987-992.
2. J. Xinmin, W. Xiaoqi, G. Wu, and Z. Weibin, Crystalline Form I of Lonidamine, Preparation Method Thereof and Composite Containing The Same. CN 101735151 B, 2012.
3. I. Bruno, J. Cole, J. M. Lommerse, R. S. Rowland, R. Taylor and M. Verdonk, *J. Comput. Aided Mol. Des.*, 1997, **11**, 525-537.
4. C. F. Macrae, P. R. Edgington, P. McCabe, E. Pidcock, G. P. Shields, R. Taylor, M. Towler and J. van de Streek, *J. Appl. Crystallogr.*, 2006, **39**, 453-457.
5. C. F. Macrae, I. J. Bruno, J. A. Chisholm, P. R. Edgington, P. McCabe, E. Pidcock, L. Rodriguez-Monge, R. Taylor, J. van de Streek and P. A. Wood, *J. Appl. Crystallogr.*, 2008, **41**, 466-470.
6. I. J. Bruno, J. C. Cole, P. R. Edgington, M. Kessler, C. F. Macrae, P. McCabe, J. Pearson and R. Taylor, *Acta Crystallogr. B*, 2002, **58**, 389-397.
7. J. Szegezdi and F. Csizmadia, A method for calculating the pKa values of small and large molecules. In *American Chemical Society Spring Meeting, March 25-29th*, ed.; Chicago, Illinois, USA, 2007.
8. ChemAxon, *MarvinSketch 16.4.25*, 2016 (http://www.chemaxon.com).

9. X. Gong, S. M. Burbridge, A. C. Lewis, P. Y. D. Wong and P. Linsdell, *Br. J. Pharmacol.*, 2002, **137**, 928-936.
10. Rigaku, *CrystalClear-SM Expert 3.1 b27*, 2013.
11. *CrysalisPro*, Agilent Technologies: Oxfordshire, 2013.
12. G. Sheldrick, *Acta Crystallogr., Sect. A: Found. Adv.*, 2015, **71**, 3-8.
13. G. M. Sheldrick, *Acta Crystallogr.*, 2008, **A64**, 112-122.
14. O. V. Dolomanov, L. J. Bourhis, R. J. Gildea, J. A. K. Howard and H. Puschmann, *J. Appl. Crystallogr.*, 2009, **42**, 339-341.